22 Chapter

Systematic Approach to Interpretation of CT of the Chest

Rubal Patel, Rakesh Shah, Sabiha Raoof, Suhail Raoof

INTRODUCTION

Computed tomography (CT) was discovered independently by Sir Godfrey Hounsfield and Dr Alan Cormack in the 1970s and has undergone substantial advancement corresponding to the progression of modern computer technology. CT has become a fundamental part of clinical decision making. Technological developments in CT have significantly influenced the diagnostic approach to many clinical diseases. This chapter focuses on a comprehensive review of the diagnostic and interpretative findings seen on CT imaging. It is broken down into three general parts: (1) the technical aspects of CT imaging with a summary of the special features and clinical indications of each technique; (2) normal components of the pulmonary parenchyma, airways and pulmonary vasculature with descriptions of specific radiographic signs pertaining to each component; (3) diseases involving the tracheobronchial tree, pulmonary parenchyma, mediastinum and a few miscellaneous conditions.

TECHNICAL ASPECTS

In general, CT provides comparatively more information than plain radiography. It provides good contrast between tissues allowing for detection of even subtle differences between tissues. Plain radiographs detect differences in contrast of about 5%, whereas CT can detect differences of less than 0.5%. Images on CT are free of superimposition of structures, thereby eliminating the effects of overlapping anatomy. Images can be obtained rapidly with a wide field of view and an ability to provide cross-sectional images of the thorax. CT can localize diseases seen on conventional radiography, assist in guidance of interventional procedures, contribute new information or detect unsuspected abnormalities.

Disadvantages of CT include the exposure to more radiation that plain chest radiography, requirement of patient transport to the CT scanner, which may be difficult in critically ill patient, and the risk of intravenous contrast administration. The wide range of indications for CT and unlimited variation of pathologic presentations make it essential to alter each CT examination to the clinical diagnosis in question. There are several technical parameters such as slice thickness, scan times, pitch, reconstruction intervals and window settings that can be selected. In general, three modes of CT imaging are currently in practice: (1) conventional CT, (2) high-resolution CT and (3) volumetric or spiral/helical CT.

Conventional CT

Conventional CT provides multiple contiguous cross-sectional images (greater than 2 mm thick) through the thorax while the patient is stationary with table position incremented between acquisitions. Narrower collimation of 5 mm may be utilized when scanning through the hilar regions; 1–2 mm to demonstrate small pulmonary nodules and high resolution CT of lung parenchyma. The conventional CT is broadly accepted and available for the work-up of many pulmonary conditions. Disadvantages of the conventional CT are motion artifact and loss of detail from volume averaging.

Multislice CT

Multislice CT has largely replaced single slice scanners and allows for extended anatomic coverage and shorter examination times.[1] Several 100-image slices are generated in less than a minute. Depending on the type of a multislice CT scanner, images can be scanned up to 64 times faster than single slice CT scanners. Consequently, they can cover more patient length per unit time, a predetermined scanning volume, or the same volume in the same time with thinner slices. The entire chest can be scanned in less than 10 seconds. There is improved temporal and spatial resolution with thinner sections and greater contrast enhancement. Diagnosis of vascular abnormalities such as subsegmental pulmonary emboli, characterization of small pulmonary nodules and recognition of airway disease are significantly improved. The distribution and morphology of diffuse lung disease is better illustrated with 1 mm collimation, can be viewed in the coronal and sagittal planes.

Reconstruction images are created by workstations that have a range of computer software programs and processing tools, which determine the quality or characteristics of the image. The reconstruction of CT data sets obtained on multislice scanners may result in several (1,000–5,000) images per examination. This makes it difficult to extract all the information presented by using standard two-dimensional techniques. Postprocessing volume imaging and 3D image display are crucial to volume visualization. Various software and workstation designs are available to improve volume visualization. Techniques such as volume rendering and maximum intensity projection, which are computer-implemented algorithms, are used to transform serially acquired axial CT image data into 3D images.

High-resolution CT

High-resolution CT (HRCT) shows very thin (less than 2 mm) cross-sectional images at 10 mm or 20 mm intervals (noncontiguous) with high spatial resolution, allowing for detailed analysis of lung structure. This provides more details than conventional CT scanning. The basic lung unit that is visible on HRCT is the secondary pulmonary lobule, around which many pathologic processes can also be visualized.[2] HRCT is particularly helpful in the detection of metastatic lesions, solitary pulmonary nodules (SPNs), bronchiectasis and characterization of interstitial lung diseases, where detailed assessment is necessary.[3] It can provide an accurate assessment of the configuration, distribution, and even the degree of disease activity and potential reversibility of diffuse lung disease. HRCT scans provide a good correlation between radiographic and histopathologic appearances. The pattern of scanning may be specified to the suspected diagnosis. For instance, scanning should be performed at 1 cm intervals for diffuse lung disease but should be limited to the involved area in focal lung diseases and SPNs.

Helical (Spiral or Volumetric) CT

Helical (spiral or volumetric) CT scanning is one major technical development in CT scanning. It provides multiplanar images of the entire chest during a single breath-hold (8–10 sec), while the patient is moved continuously through the CT gantry with continuous rotation of the X-ray tube and detector assembly. The main advantages include speed, less radiation exposure, and an ability to retrospectively construct 3D images. Respiratory motion is eliminated and volumetric data can be manipulated to obtain overlapping axial sections without additional radiation to the patient.[4] However, the requirement for breath-holding may not be feasible for patients with symptomatic pulmonary disease. It is useful in the evaluation of mediastinal abnormalities.

CT Angiography

CT angiography is obtained during a 15–30 second helical scan. The influx time of the contrast medium and the degree of vascular and parenchymal enhancement are dependent upon the concentration of contrast material, the rate of injection, and the cardiac output. It is exceedingly effective in diagnosis of pulmonary embolism. Several studies have confirmed comparable results of CT angiography to conventional pulmonary angiography.

Low-dose CT

Low-dose CT limits the radiation exposure to the patient and produces high-resolution three dimensional images. It is indicated for use in screening for lung cancer in high-risk populations.[5] The radiation dose of a low-dose CT scan is equivalent to approximately 15 chest X-rays and five times lower than the dose from a conventional CT scan. The disadvantage of low-dose CT is higher false positive results.

The special features, advantages and disadvantages and clinical indications of these techniques are summarized in **Table 1**.

NORMAL COMPONENTS OF PULMONARY PARENCHYMA

A good knowledge of lung anatomy is necessary to understand the CT features of lung diseases. It allows for better understanding of the pattern of disease as well as the specific distribution in the lung. The lung is composed of anatomical elements of similar architecture at gradually smaller sizes. These include lungs, lobes, segments, subsegments, secondary lobules and acini. Each division is organized around central supporting structures such as airways and arteries and peripheral supporting structures such as pleura and connective tissue septa.[6]

The support system of the lung consists of a network of connective tissues, which forms the interstitium. This structure not only maintains a strong structural support for the airways, blood vessels and alveoli, but also is thin enough to allow for gas exchange. The interstitium can be divided into three components that communicate freely: (1) the peripheral, (2) axial and (3) parenchymal connective tissue[7] **(Fig. 1)**. The peripheral connective tissue extends from the lung pleura to the lung septa. The septa are incomplete partitions within the lung that divide the lung segments, subsegments and secondary pulmonary lobules and acini. The axial connective tissue stems from the hilum and surrounds the bronchovascular structures, extending peripherally. The parenchymal connective tissue is located in between the alveoli and capillaries, where gas exchange takes place. It extends to the axial and peripheral connective tissues.[7]

The normal segmentation of pulmonary lobes includes three (upper, middle and lower) in the right lung and two (upper and lower) in the left lung. They are separated by interlobar fissures. Lobes are identified on CT by visualization of interlobar fissures or an avascular plane on which they lie or by identifying bronchial branches that lead to the

Table 1 Clinical indications, special features, advantages and disadvantages of various techniques of CT chest imaging

CT technique	*Indications*	*Special features*	*Advantages/Disadvantages*
Conventional	Work-up of many pulmonary conditions: • Localization and characterization of mediastinal mass • Staging of lung cancer • Detection of pulmonary metastases • Approach for biopsy	• Provides multiple contiguous cross-sectional images • Allows for scanning throughout the thorax	• Susceptible to motion artifact • Loss of detail from volume averaging
Multislice	Diagnosis of vascular abnormalities: • Subsegmental pulmonary emboli • Characterization of small pulmonary nodules • Evaluation of airway disease	• Improved resolution • Improved contrast enhancement • Ability to create retrospective reconstructions • Thinner sections	• Faster imaging • Less motion artifacts • Greater anatomic coverage
HRCT	Evaluation and detailed characterization of: • Solitary pulmonary nodule • Interstitial lung disease • Bronchiectasis • Metastatic lesions	• Thinner cross-sectional images • Provides more detail than conventional CT scanning	• Accurately assessment of the pattern and distribution of diffuse lung disease • Characterization of disease activity • Guidance for lung biopsy • Does not provide contiguous images–skips areas between the thin sections
Helical	Evaluation of various thoracic injuries: • Aortic dissection • Pneumothorax • Pulmonary contusions and lacerations • Tracheobronchial injury • Skeletal injuries such as rib, sternal, vertebral fractures • Diaphragmatic injuries	• Increased scanning speed • Improved vascular enhancement • Thinner collimation • Acquires volumetric data of the thorax, allowing for manipulation of image data • Able to generate high quality multiplanar 2-D and 3-D reconstructions	• Capable of scanning large volumes of tissue during a single breath hold • Minimizes motion artifact • Generates high quality images with the ability to show branching or oblique airway or vascular anatomy • Assists in surgical planning
CT Angiogram	Detection and evaluation of vascular abnormalities: • Aortic disease • Pulmonary embolism	• Requires rapid intravenous injection of contrast material • Ability to use volume rendering to improve diagnostic accuracy • Technical details may be manipulated to obtain optimal vascular studies	• Proper injection timing is essential to ensure imaging at the time of peak intravascular enhancement • The volume of contrast used should be adequate to maintain maximal vascular opacification throughout the spiral acquisition • With optimal technique, CT angiography can provide accurate images, eliminating the need for conventional angiography
Low-dose CT	Used for lung cancer screening	• Reduced radiation dose	• Faster scanning speed • Loss of detail • Increased false positive results

corresponding lobes.[8] Pulmonary segments and subsegments are not as easily discerned as lobes. Of the three units of lung structure, i.e. the primary pulmonary lobule, acinus and secondary pulmonary lobule, the secondary lobule is the smallest unit of lung structure that is seen on HRCT bordered by interlobular septa[9] **(Figs 2 and 3)**. The secondary lobules are the building blocks around which CT patterns are constructed. These structures are extremely important in the interpretation of lung changes seen on CT.

The interpretation of HRCT is exceptionally useful for the diagnosis of various diffuse and focal lung diseases, which are centered around the secondary pulmonary lobule. Therefore a good knowledge of the anatomy of the secondary lobule is essential to determine the distribution pattern of the disease. Differential diagnosis of lung disease can be limited by evaluation of whether the disease is located in or around the airways, the blood vessels, the lymphatics or the lung interstitium.[10]

Secondary Pulmonary Lobule

The secondary pulmonary lobules are polyhedral in shape and differ in size from 1.0 cm to 2.5 cm and are formed by a collection of acini.[2,7,10] The reported number of acini that

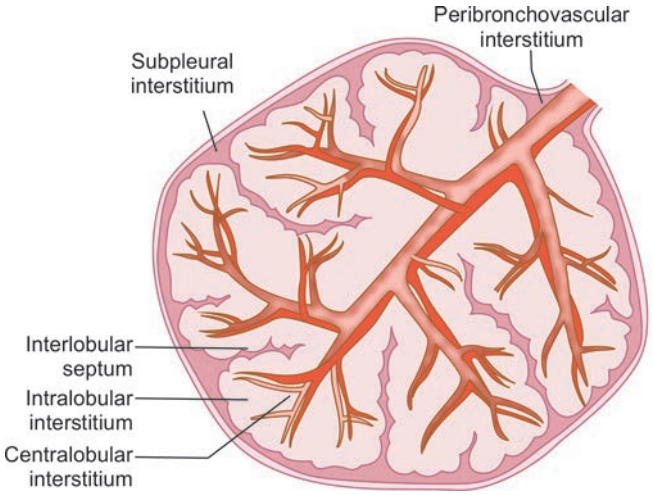

Fig. 1 Divisions of the pulmonary interstitium. The interstitium can be divided into three components that communicate freely: the peripheral, axial and parenchymal connective tissue. The peripheral support system consists of the subpleural and interlobular septa. The axial support system consists of the peribronchial and centrilobular interstitium

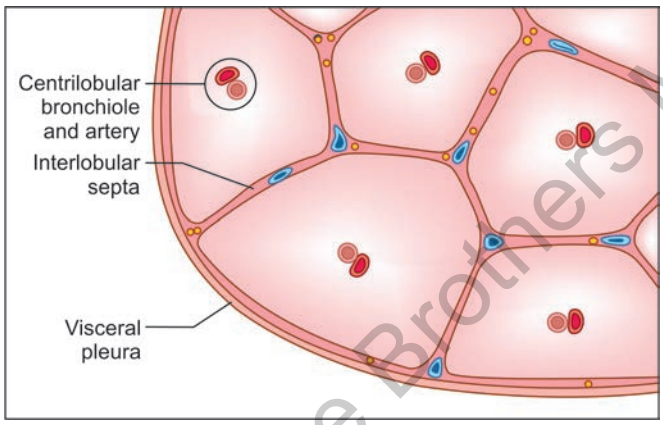

Fig. 2 The secondary pulmonary lobule. The central structures include the intralobular pulmonary artery and terminal bronchiole. The septal structures include the pulmonary venules, lymphatics and fibrous septa

Fig. 3 HRCT chest performed at the lung base, showing interlobular septal thickening (arrow), reticular opacities and some honeycombing changes

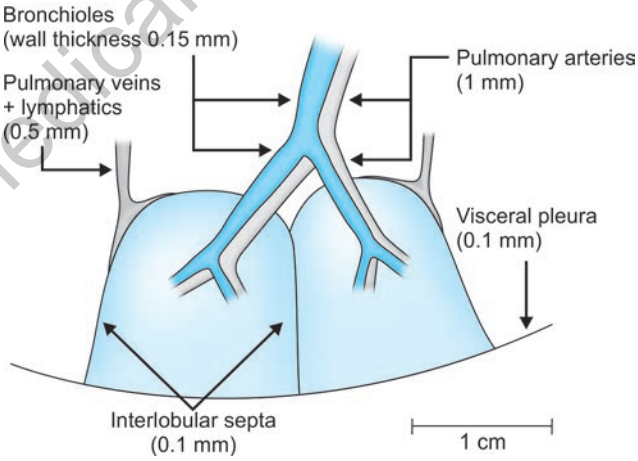

Fig. 4 The secondary pulmonary lobule. Each secondary lobule is made up of a small bronchiole and pulmonary artery and bordered by interlobular septa, where a pulmonary vein and lymphatic branches reside[10]

Source: Raoof S, Amchentsev A, Vlahos I, et al. Pictorial essay: mulitinodular disease: a high-resolution CT scan diagnostic algorithm. Chest. 2006;129(3):805-15.

form a secondary pulmonary lobule vary considerably and a range of 3–12 has been described. An acinus is the largest lung unit where all airways participate in gas exchange. Each secondary lobule is made up of a small bronchiole and pulmonary artery and bordered by interlobular septa, where a pulmonary vein and lymphatic branches reside **(Fig. 4)**.[10,11]

Interlobular Septae

The secondary lobules are surrounded by interlobular septae made by connective tissue. The lymphatic system draining the visceral pleura, courses within the interlobular septae along with the septal veins leading to the lymphatics and nodes within the hila. The interlobular septae measure 0.1 mm in the subpleural location, are much thinner and less defined in the center.[2] The thickness of the peripheral interlobular septa is at the lower limit of HRCT resolution, hence may or may not always be seen, especially in CT scans of normal patients.

Centrilobular Region

The central part of the secondary lobule contains the peribronchovascular interstitium that surrounds the terminal pulmonary artery and the terminal bronchial branches.[10]

It is difficult to discern the bronchial or arterial structures and the HRCT appearance of these structures is dependent on their size. A linear branching or dot-like opacity usually seen within the center of the lobule represents the intralobular artery branch and its distributions.[2] The centrilobular arteries are not seen to extend to the pleural surface. The airway wall thickness determines the visibility on HRCT. The wall thickness of a normal terminal bronchiole measures 0.1 mm, which is below the resolution of HRCT.[12] Therefore on HRCT imaging, intralobular bronchioles are not usually identified, and not normally seen within 1 cm of the pleural surface.

Specific Signs

The diagnostic approach for HRCT relies upon a good understanding of lung anatomy in general, particularly the secondary pulmonary lobule, the pattern and the distribution of disease, and on associated findings such as pleural plaques, calcifications, thickening, effusions, lymph node enlargement, and the clinical history.

The principal parenchymal patterns seen on HRCT include "reticular and nodular structures, increased opacity (ground-glass and air space filling or consolidation), and decreased opacity, including cystic lesions, mosaic attenuation, and air trapping".[6] Accompanying findings include linear opacities, parenchymal bands and architectural distortion **(Fig. 5)**.

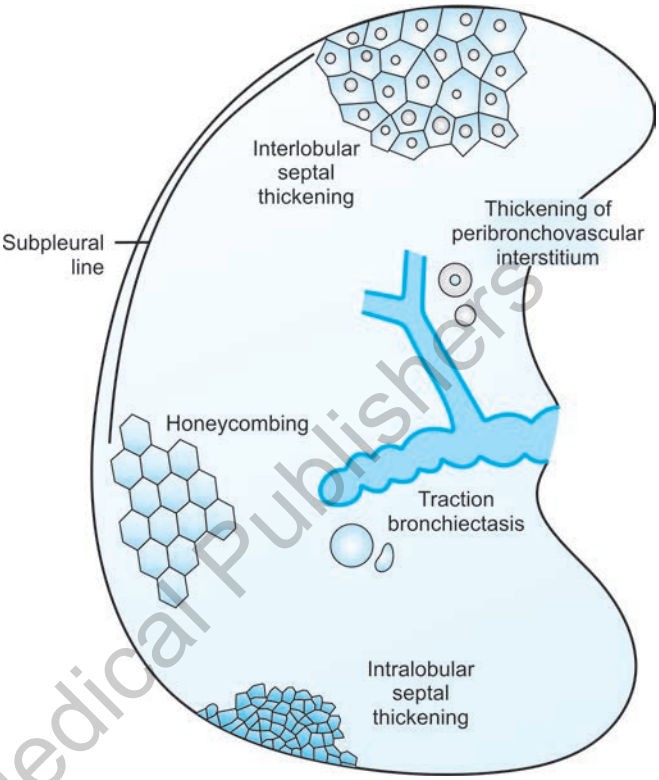

Fig. 5 Pictorial representation of reticular opacities: Thickening of the peribronchovascular interstitium, interlobular septal thickening, honeycombing and traction bronchiectasis

Reticular Patterns

Reticular opacities occur with thickening of the pulmonary interstitium by fluid, fibrosis, or other infiltrative processes **(Fig. 6)**. The reticular pattern can be coarse, intermediate or fine. The coarse reticular pattern (1 cm) occurs due to thickening of interlobular septae, intermediate reticular changes are seen with honeycombing, and fine reticular changes are seen with intralobular septal thickening. The reticular pattern may be smooth, nodular or irregular.

Interface sign: The interface sign is the most common and earliest HRCT abnormality found in interstitial disease with an irregular and thickened appearance of the normally smooth septae bordering the parenchyma with vessels, bronchi and visceral pleura.[6] This is, however, a nonspecific sign of interstitial diseases. Other findings include interlobular septal thickening, peribronchial thickening, intralobular linear opacities and cysts.

Interlobular septal thickening: Interlobular septal thickening is a characteristic finding of interstitial lung disease. They appear as 1–2 cm lines that are perpendicular to the pleura and extend out to the pleural space. Centrally they form polygonal structures outlining the secondary lobules **(Figs 3 and 5)**.

Peribronchial or perivascular interstitial thickening: Peribronchial or perivascular interstitial thickening results from thickening of the connective tissue surrounding the bronchi or pulmonary vessels. The thickening may be smooth or irregular. Dilatation of the bronchi may result in cases where surrounding fibrosis results in traction, known as traction bronchiectasis **(Figs 5 and 7)**.

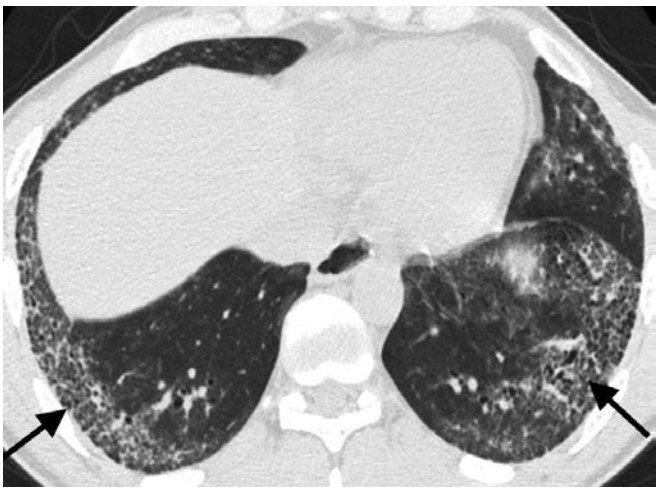

Fig. 6 HRCT through the lung bases showing subpleural reticulation in a patient with idiopathic pulmonary fibrosis. Also visible are small cysts (arrows) from honeycombing

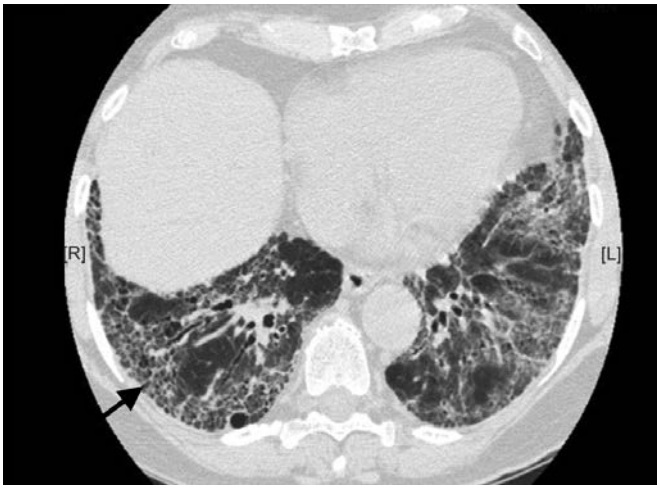

Fig. 7 HRCT through the lower lung zones showing honeycombing (arrow) with dilated non-tapering bronchi especially on the right side (traction bronchiectasis) and architectural distortion

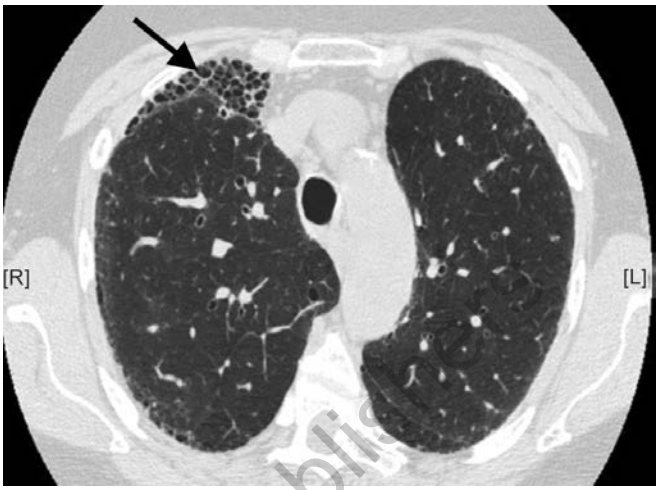

Fig. 8 HRCT through the upper lung zones demonstrating numerous cysts (arrow) involving the subpleural regions resulting in honeycombing. Note dilated bronchi adjacent to branches of the pulmonary artery

Intralobular linear opacities: Intralobular linear opacities occur with thickening of the interstitium within the secondary pulmonary lobule. This forms a fine reticular pattern with small irregular lines separated by only a few millimeters. This pattern is most commonly caused by fibrosis. The distribution (upper vs lower lobes) and associated findings vary with different diseases.

Cysts: Cysts are rounded air-containing spaces surrounded by well-defined walls. When they are 4–5 mm in size and present in the subpleural region, they represent honeycombing in end-stage fibrosis and are associated with traction bronchiectasis and architectural distortion **(Figs 8 and 9)**.

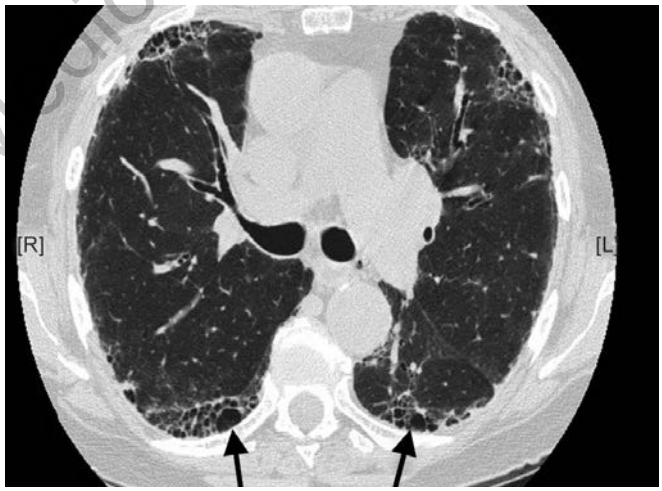

Fig. 9 HRCT demonstrating cystic changes in the subpleural regions (arrows) resulting in a honeycombing pattern in a patient with idiopathic pulmonary fibrosis. Note dilated bronchi (right upper lobe dilated bronchi) and paucity of ground glass opacity

Nodules

Nodules less than 1 cm may be seen in several acute and chronic infiltrative lung diseases. Nodular patterns include airspace lesions with ill-defined or ground-glass borders, and interstitial nodules with sharp, hazy, or stellate margination.[8] The distribution of nodules is useful in narrowing the differential diagnosis.[11] Nodules may predominantly follow a perilymphatic, centrilobular or random distribution. The perilymphatic nodules are found along the bronchovascular interstitium, interlobular septa and subpleural areas. Centrilobular nodules are usually poorly defined and are seen in the center of the secondary lobule. Random nodules occur due to hematogenous spread and thus well-defined and randomly situated in the lung.

Increased Opacities

Ground glass opacification: A ground glass opacity refers to the presence of either a "focal or diffuse and hazy", increased attenuation of the lung, which does not obscure the vascular or bronchial structures, and not associated with air-bronchograms[13,14] **(Figs 10 and 11)**. It is caused by partial filling of the air-space. Although ground glass attenuation is a nonspecific sign, it represents an active process, which may potentially be treated or reversed.[15]

Consolidations or airspace filling defects: Parenchymal consolidation or airspace filling causes opacification with obscuration of vascular structures accompanied by air bronchograms. These two features differentiate it from ground-

Fig. 10 HRCT through the basilar lung showing areas of extensive ground glass attenuation, honeycombing and peribronchial thickening

Fig. 12 CT chest through mid-lung showing bilateral dense opacity with air bronchograms. This is typical of air space disease

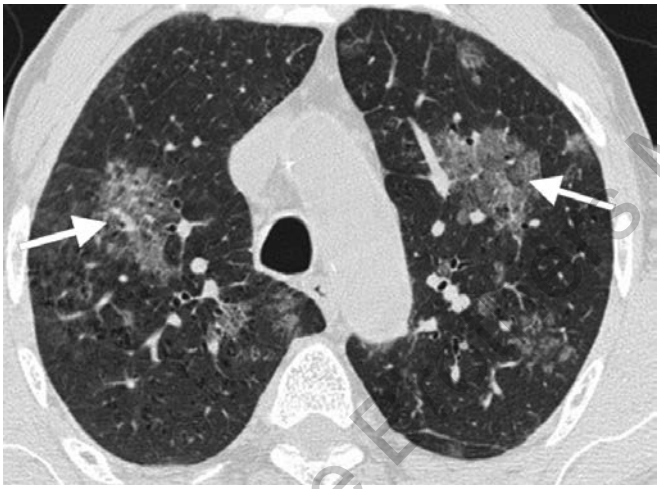

Fig. 11 High resolution CT scan of the upper lung zone demonstrating patchy ground glass attenuation (arrows) in a patient with desquamative interstitial pneumonia

Fig. 13 HRCT chest at the level of the main stem bronchi illustrating dense bilateral opacities in a peripheral distribution. The patient had chronic eosinophilic pneumonia

glass changes **(Figs 12 and 13)**. These changes result from replacement of alveolar gas by pus, edema, blood, or cells.[15]

Decreased attenuation: Decreased lung attenuation can occur from lung damage, e.g. emphysema or diminished blood flow, e.g. pulmonary vasculature or airway abnormalities.

In emphysema, areas of abnormally low attenuation develop that may have no identifiable walls **(Figs 14 and 15)**.[16] There are three main forms of emphysema: (1) centrilobular, (2) panlobular, and (3) distal acinar emphysema.

Low-attenuated areas may also result from decreased perfusion arising from blood flow redistribution in vascular obstruction or airway abnormalities. Redistribution of blood flow away from areas of vascular obstruction or airway obstruction leads to increased attenuation in areas of normal lung parenchyma. This pattern of variable regional areas of decreased and increased attenuation due to regional differences in perfusion is termed mosaic attenuation **(Fig. 16)**.[12] The two processes, i.e. vasculature versus airway abnormalities may be differentiated by performing expiratory CT.[17] Airway disease will show no change in the lucent areas where there is air trapping, whereas in primary vascular disease, the attenuation in both the hyperlucent and hypolucent areas will increase equally on end expiration.

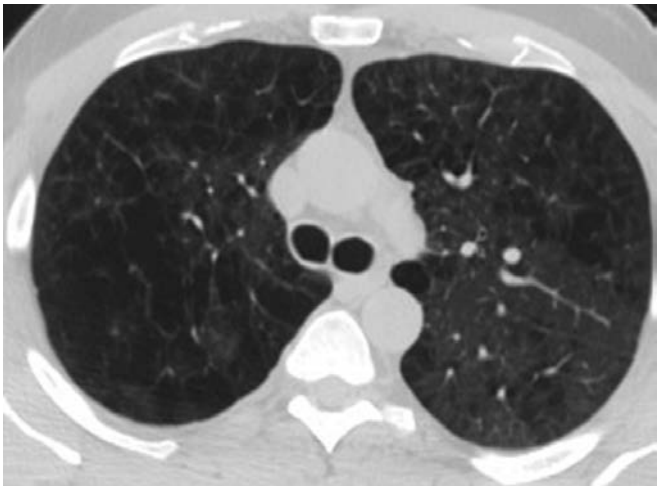

Fig. 14 CT chest through the upper lobes showing focal areas of decreased attenuation. No definable walls are visible in these focal areas of hyperlucency. This patient was a smoker with centrilobular emphysema

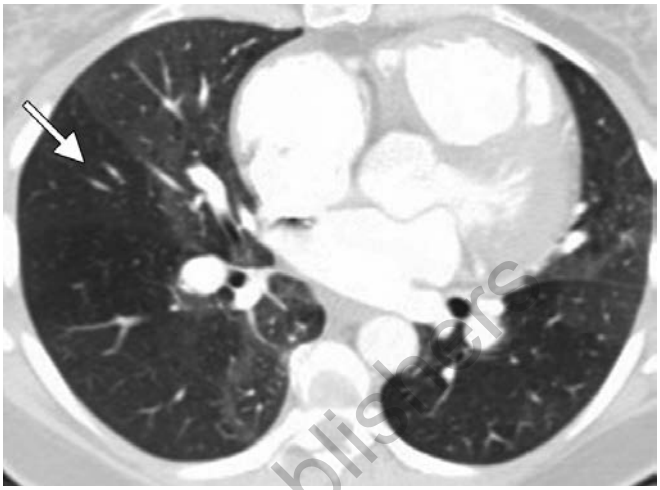

Fig. 16 CT chest through the lower lobes demonstrating a pattern of variable regional areas of decreased and increased attenuation, also known as mosaic attenuation. This patient had chronic thromboembolism. Note the decreased vascularity in the hypolucent areas of the lung (arrow)

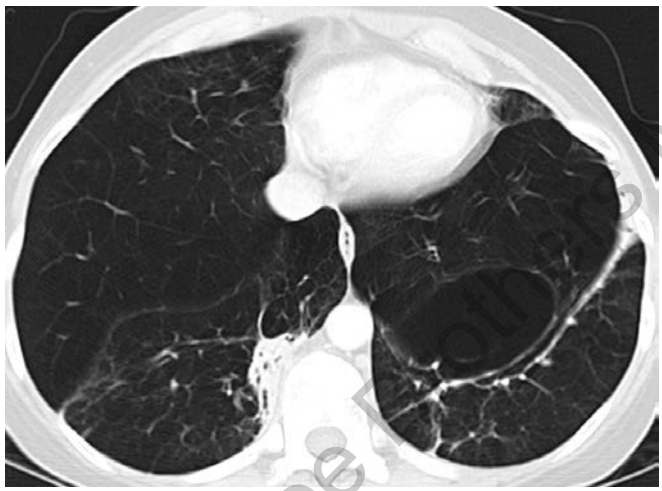

Fig. 15 CT chest through the lower lobes showing extensive panlobular emphysema in a patient with alpha 1 antitrypsin deficiency
Courtesy: Dr A Soleh

Differentiation of mosaic attenuation (due to blood flow redistribution) from true ground-glass attenuation can be accomplished by evaluating the vessel size in the increased and decreased areas. In infiltrative lung disease, the vessel size and number will be equal in areas of increased and decreased attenuation. In airways or vascular disease, vessel size and number will be decreased in regions of hypoattenuation.[17] These findings are summarized in **Table 2**.

NORMAL LUNG COMPONENTS OF THE AIRWAYS

The airways divide by asymmetric dichotomous branching with approximately 23 generations of branches from the trachea to the alveoli that become thin walled as they branch. The accuracy of CT to evaluate the central airways is well established.[18]

Table 2 Differential diagnosis of mosaic attenuation

Abnormality	*Causes*	*Caliber of vessels*	*Effect of exhalation*
Small airways disease	• Asthma • Bronchiolitis obliterans • Cystic fibrosis	Decreased size and number of vessels in hypo-attenuated areas due to regional air trapping and hypoxic vasoconstriction	Unequal attenuation in the hyperlucent and hypolucent areas No change in hypolucent areas (air-trapping)
Small vessel disease	• Chronic pulmonary embolism	Decreased size and number of vessels in hypo-attenuated areas due to obliteration of small vessels	Attenuation in both the hyperlucent and hypolucent areas will increase equally (no air-trapping)
Infiltrative disease	• *Pneumocystis jiroveci* pneumonia • Eosinophilic pneumonia • Hypersensitivity pneumonia	Equal size and number of vessels in areas of increased and decreased attenuation	Attenuation in both the hyperlucent and hypolucent areas will increase equally (no air-trapping)

Trachea

The trachea is a cartilaginous structure extending from the inferior border of the cricoid to the carina. It may be divided into extrathoracic and intrathoracic segments along the manubrium and is approximately 10–12 cm in length.[19] There are 16–22 cartilaginous horseshoe-shaped rings that form the trachea anteriorly. The posterior portion of the trachea consists of a thin fibromuscular membrane, without cartilage. The blood supply to the trachea comes superiorly from the branches of inferior thyroid artery and right intercostal artery and inferiorly from the bronchial arteries and third intercostals artery. The cross-sectional appearance of the trachea may be oval, rounded or horseshoe shaped **(Fig. 17)**. The average tracheal diameter in men is 19.5 mm and in women 17.5 mm.[20] The shape of the trachea may vary with expiration, resulting in a crescentic shape during forceful expiration, due to posterior tracheal bowing.[21]

The trachea splits into main bronchi, which divide into lobar bronchi. The lobar bronchi divide into segmental bronchi, which ultimately branch into subsegmental bronchi. After several more divisions at this level, the terminal bronchi emerge to give rise to the bronchioles.

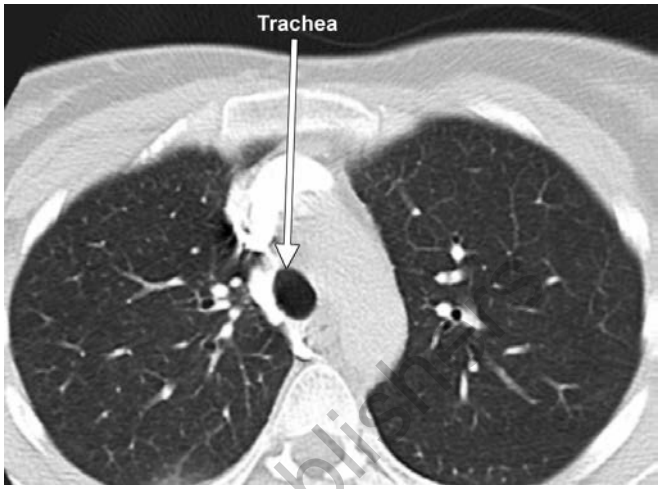

Fig. 17 CT chest through the upper lobes demonstrating normal oval tracheal lumen during inspiration

Bronchi

The bronchi are also composed of cartilaginous and fibromuscular structures but the distribution is less regular than the trachea. They become more difficult to see in the periphery of the lung. Bronchi contain cartilage and glands within their walls, unlike bronchioles. Bronchioles can be divided into membranous bronchioles, which solely conduct air, and respiratory bronchioles, which have alveoli in their wall and are involved in gas exchange. Bronchioles along with corresponding pulmonary artery branches lie within the center of the secondary pulmonary lobule.

Evaluation of the airways should be done using spiral CT technique with thin collimation. The ability of CT to image a particular bronchus depends on its size and orientation relative to the scan plane. The main bronchi and bronchus intermedius are easily detected due to their large size. The origin of the proximal lobar and segmental bronchi can also be identified in most cases. **Table 3** illustrates the nomenclature of the bronchial tree.[22] **Figures 18 to 24** illustrate the division of the bronchial anatomy as seen on spiral CT. The bronchi and large arteries usually run together, with their diameter of approximate equal size. In general, airways less than 2 mm in diameter or close to 1–2 mm to the pleural surface are below the resolution of HRCT images.[2] The presence of visible bronchial structures in the lung periphery signifies pathologic thickening or ectasia.

Specific Signs

Saber-sheath Trachea

A saber-sheath trachea is a condition with marked reduction in the transverse diameter of the intrathoracic trachea greater than half of the sagittal diameter **(Fig. 25)**. It results from conditions such as chronic obstructive pulmonary disease.[23]

Tracheobronchomegaly

Tracheobronchomegaly results when the tracheal diameter increases and can be due to congenital or acquired disease **(Fig. 26)**.[24] It is also known as Mounier-Kuhn syndrome

Table 3 Nomenclature of the bronchial tree

Right lung				*Left lung*		
Lobes	*Upper*	*Middle*	*Lower*	*Upper*		*Lower*
Segments	Apical	Lateral	Superior	Upper division	Lower (Linguar division)	Superior
	Posterior	Medial	Medial basal	Apical posterior	Superior	Anterior-medial basal
	Anterior		Anterior basal Lateral basal Posterior basal	Anterior	Inferior	Lateral-basal Posterior-basal

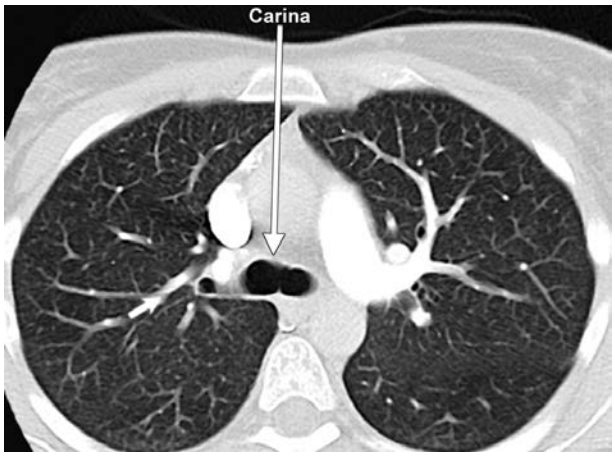

Fig. 18 CT chest showing tracheal division into the right and left main stem bronchi. Note the cross-sectional cut of the right upper lobe (thick arrow). Of note, a patchy area of hazy opacity is seen in the left upper lobe laterally

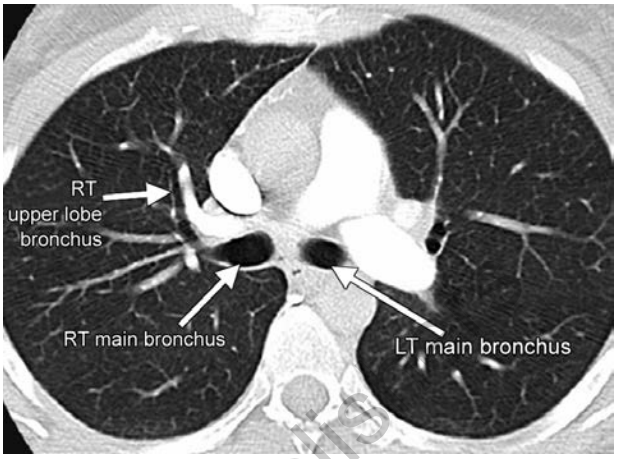

Fig. 21 CT chest showing left and right main stem bronchi with the take off of the right upper lobe bronchus

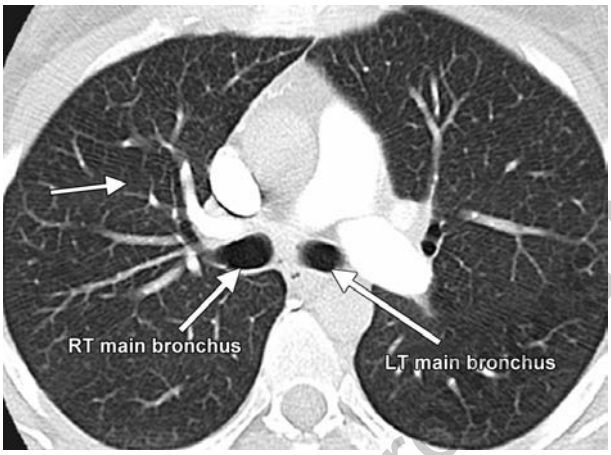

Fig. 19 CT chest showing the right and left main stem bronchi. Note the illustration of the right upper lobe (thick arrow), which almost always lies in the plane of scan

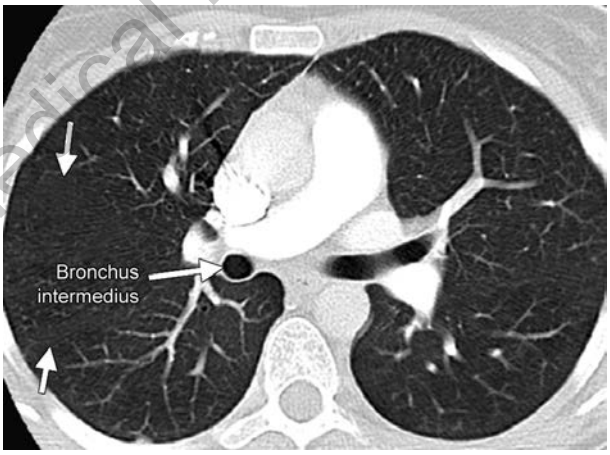

Fig. 22 CT chest illustrating a cross-sectional image of the bronchus intermedius and the left upper lobe bronchus. Note the presence of the minor fissure in the left lung, which is visible as an area with relative paucity of bronchovascular markings (thick arrows)

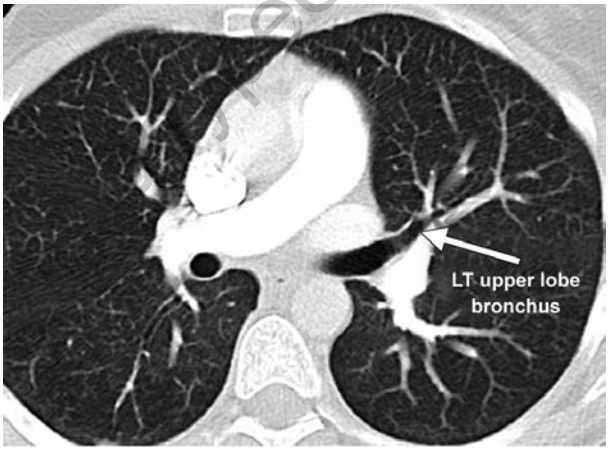

Fig. 20 CT chest at the level of the left main stem bronchus showing the left upper lobe and bronchus

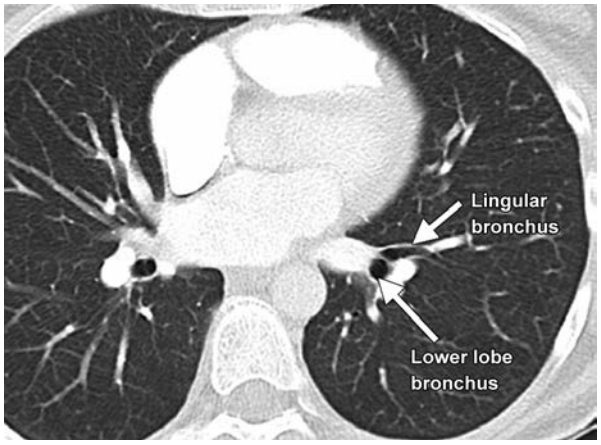

Fig. 23 CT chest showing the origin of the lingular and left lower lobe bronchus

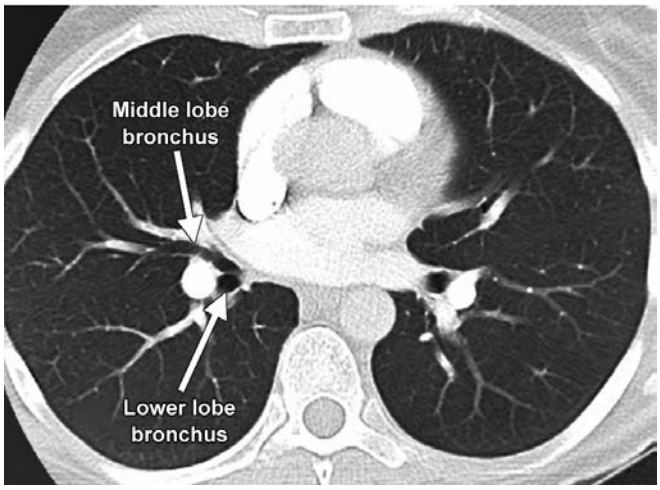

Fig. 24 CT chest illustrating right middle lobe and right lower lobe bronchi

Fig. 26 CT chest showing an increased trachea diameter, resulting in tracheomegaly or Mounier-Kuhn syndrome. The normal tracheal diameter is 19.5 mm in a male and 17.5 mm in a female

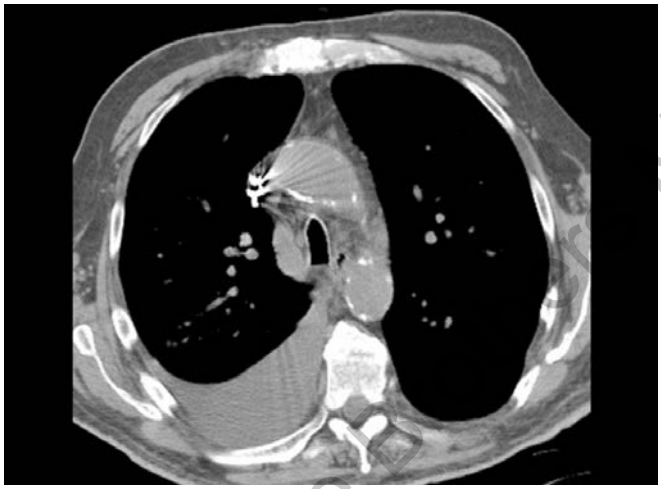

Fig. 25 CT chest showing marked reduction in the coronal diameter of the trachea as compared to the sagittal diameter indicating the characteristic appearance of a saber-sheath trachea. Of note, there is a moderate sized pleural effusion on the right

and is commonly associated with tracheal diverticulosis, bronchiectasis and recurrent infections.

Tracheal Diverticulosis

Tracheal diverticulosis results from outpouching of the posterolateral tracheal wall secondary to weakness in the trachealis muscle. It may be congenital or acquired and is associated with recurrent infections and hemoptysis.[25] On CT imaging, a small focal paratracheal air column is a classic appearance for a tracheal diverticulum.[26]

Tracheobronchopathia Osteochondroplastica

Tracheobronchopathia osteochondroplastica (TBO) is a rare benign condition of unknown etiology characterized by multiple submucosal osteocartilaginous nodules involving the trachea and main stem bronchial walls **(Fig. 27)**. On CT, there is tracheal scalloping and nodularity with irregular narrowing of the trachea. It spares the posterior tracheal membrane.[27]

Tracheobronchomalacia

Tracheobronchomalacia (TBM) is a common, under-recognized cause of dyspnea and cough. It is a condition that results in excessive airway collapse of the tracheal and bronchial walls. By definition, in patients with TBM, the cross-sectional area of the trachea shows a reduction of at least 50% during quiet breathing, forming a crescent-shaped airway **(Fig. 28)**. It can result from several etiologies including but not limited to external trauma, postintubation, chronic obstructive pulmonary diseases and chronic inflammatory diseases such as relapsing polychondritis. It is best diagnosed by paired inspiratory and expiratory dynamic CT imaging.[28]

Tracheal Bronchus

A tracheal bronchus is an uncommon anomaly in which an ectopic bronchus arises from the trachea above the carina. It is more common on the right but can occur on either side.[26]

Fig. 27 CT chest section through the mid-trachea showing nodularity of the trachea with calcifications and sparing of the posterior tracheal wall, a characteristic finding in tracheobronchopathia osteochondroplastica

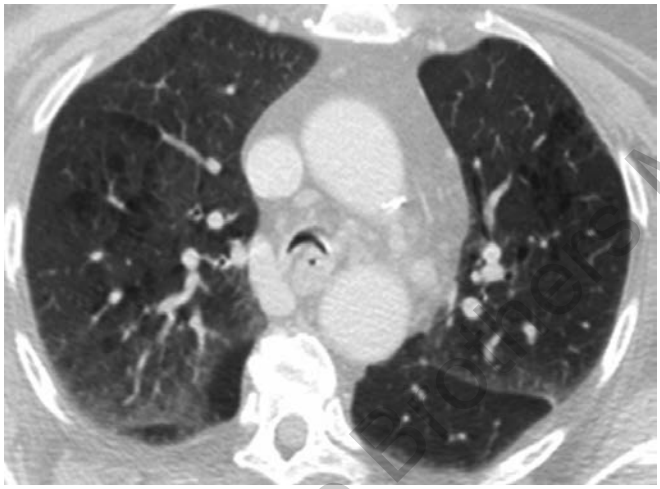

Fig. 28 CT chest in exhalation, showing excessive airway collapse with posterior bowing resulting in tracheomalacia

NORMAL LUNG COMPONENTS OF PULMONARY VASCULATURE

A comprehensive knowledge of the cross-sectional anatomy of pulmonary arteries and veins is imperative in the diagnosis of vascular abnormalities and interpretation of CT images. The arteries accompany the airways and their pattern of division is similar to the branching of airways.

Pulmonary Arterial Anatomy

The main pulmonary artery begins from the base of the right ventricle and extends superiorly dividing into the right and left pulmonary arteries. These central pulmonary arteries are intrapericardial. Pulmonary arteries are elastic and thin-walled vessels.

The main pulmonary artery on CT is the most anterior vascular structure arising from the heart. It is slightly smaller than the ascending aorta in normal subjects, measuring on average 28 mm in diameter.[29] This measurement is best taken at its bifurcation, lateral to the aorta in the short axis of the pulmonary artery. CT measurements of the pulmonary artery have been shown to correlate with pulmonary artery pressure.[29]

The main pulmonary artery divides lateral to the ascending aorta into the right and left pulmonary arteries. The right pulmonary artery arises nearly at a right angle and passes posteriorly to the ascending aorta and anteriorly to the right main bronchus as it crosses the mediastinum. It is seen along its length on CT since it lies in the scan plane. The left pulmonary artery appears in direct communication of the main pulmonary artery. It passes slightly to the left of its origin and arches over the left main bronchus as it enters the hilum. The right and left pulmonary arteries are usually of equal size.

Similar to bronchial division, the pulmonary arteries divide by dichotomous branching. There are approximately 17 divisions from the bifurcation of the main pulmonary artery to arteries of a diameter of 10–15 mm.[30]

The right main pulmonary artery divides into an ascending trunk, truncus anterior, primarily supplying the right upper lobe, and a descending trunk, interlobar branch, supplying mainly the right middle and lower lobes. The left pulmonary artery continues as the descending or interlobar left pulmonary artery, giving rise to segmental branches of the left upper and lower lobes **(Fig. 29)**. The branching of the lobar, segmental and subsegmental pulmonary artery branches show considerable variation and are sometimes identified by associated bronchi. Occlusion of segmental pulmonary arteries can be easily identified on CT, whereas subsegmental pulmonary arteries occlusion may not always be visualized.

Pulmonary Veins

The pulmonary veins arise from alveolar capillaries where pulmonary venules form. Pulmonary veins run through the interlobular septa and then through the more central connective tissue sheaths to the left atrium.[31] The branching patterns of veins are more variable; generally two superior and two inferior pulmonary veins are found on each side.

Bronchial Arteries

The bronchial arteries belong to a different arterial system that originates from the systemic circulation. They accompany the bronchi to the level of the terminal bronchi, where they ramify into pulmonary plexus and are drained by the pulmonary venous system.

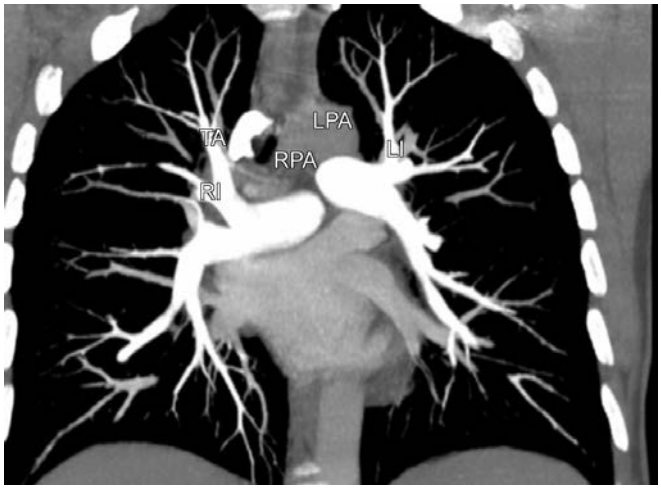

Fig. 29 Coronal image of CT chest showing normal hilar pulmonary artery branching. The right main pulmonary artery (RPA) divides into an ascending trunk, truncus anterior (TA), primarily supplying the right upper lobe, and a descending trunk, interlobar branch (RI), supplying mainly the right middle and lower lobes. The left pulmonary artery (LPA) continues as the descending or interlobar left pulmonary artery (LI), giving rise to segmental branches of the left upper and lower lobes

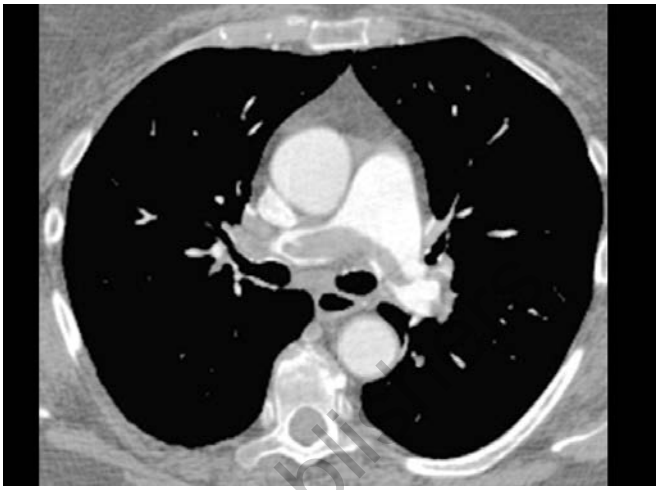

Fig. 30 CT angiogram showing a large filling defect at the division of the right and left main pulmonary arteries. This is also known as a saddle embolism. Note the acute angle formed by the embolus and the contrast-filled lumen

Abnormalities

Pulmonary Artery Agenesis

Congenital abnormalities resulting in embryonic disappearance of proximal segments of the right and the left sixth arch may result in agenesis of either the right or left pulmonary artery respectively. It may occur as an isolated condition or along with cardiac abnormalities. Features seen on CT include a small hemithorax, ipsilateral displacement of the mediastinum and absence of the analogous pulmonary artery.[32]

Anomalous Pulmonary Artery

An anomalous retrotracheal left pulmonary artery is seen on CT to arise from the right pulmonary artery, looping behind the trachea and right main stem bronchus before reaching the left hilum. This can result in symptomatic compression of the right main stem.[33]

Anomalous Pulmonary Vein

Anomalous pulmonary vein abnormalities result in drainage of blood completely or partially into the right atrium.[34] In Scimitar syndrome, there is aberrant drainage of the right pulmonary vein into the inferior vena cava.

Pulmonary Embolism

Knowledge of the hilar vascular anatomy is crucial for the recognition of an acute pulmonary embolism. The identification of pulmonary arteries is done using the bronchial anatomy as reference since the arteries tend to lie adjacent to the airways. The most consistent CT finding of pulmonary embolism is an intraluminal filling defect **(Fig. 30)**. Depending on the plane of the CT and orientation of the artery, these defects may appear as spherical, eccentric or serpiginous filling defects.[35] In large arteries, they may also appear as free-floating masses. An acute pulmonary embolus forms an acute angle with contrast-filled lumen. In chronic pulmonary embolism, the thrombi are smooth or irregular eccentric mural defects, representing organization of the thrombus.[36]

Pulmonary Artery Aneurysm

Pulmonary artery aneurysms have been associated with a spectrum of conditions, such as—in infections, congenital heart conditions, atrial and ventricular septal defects and vasculitis.[37] The primary cause of pulmonary artery aneurysm is cystic medial necrosis. A false aneurysm may be seen as also develop as a result of a pulmonary artery catheter. CT findings are often nonspecific and erroneously identified as masses, nodules or adenopathy.

Pulmonary Varix

Pulmonary varices may be easily identified on CT as an enlarged mass with aneurysmal dilatation of the pulmonary vein[38] **(Fig. 31)**.

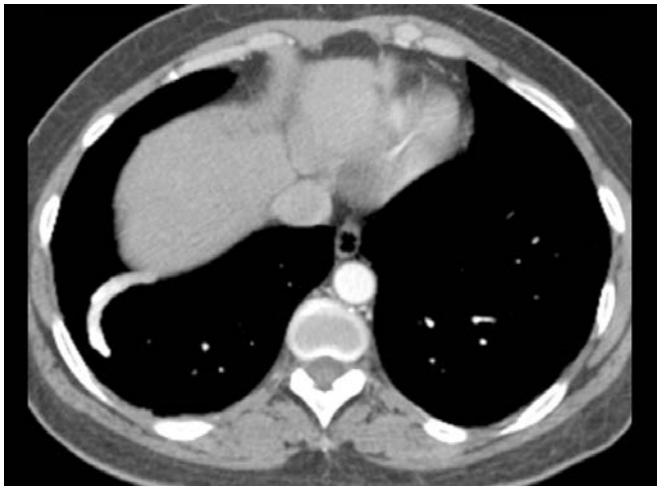

Fig. 31 CT chest with contrast showing a dilatation of the pulmonary vein from a pulmonary varix

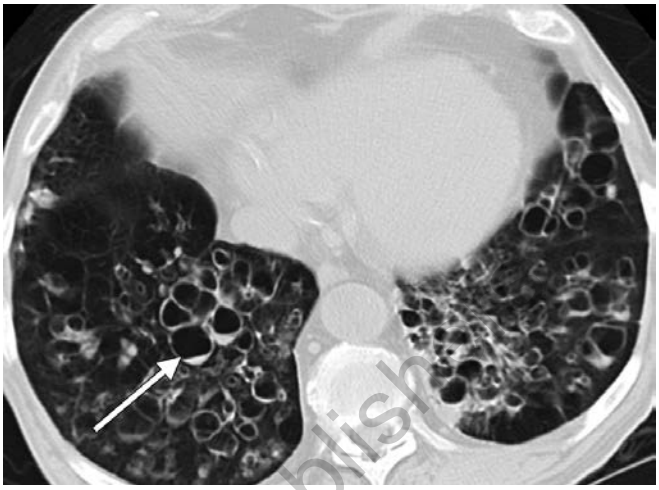

Fig. 32 CT chest through the lower lobes showing saccular bronchiectasis. Some of the bronchi have fluid (arrow) in them. This patient developed bronchiectasis from repeated childhood infections
Source: Dr A Saleh

TRACHEOBRONCHIAL DISEASES

Bronchiectasis

The definition of bronchiectasis is localized, irreversible dilatation of the bronchial tree.[39] Several conditions have been associated with bronchiectasis.[40] These include postinfectious causes following early childhood infections, tubercular sequela, allergic bronchopulmonary aspergillosis, immunodeficiency states and congenital causes. This commonly arises from acute, chronic or recurrent infections. Symptoms usually develop with severe disease and include a history of recurrent pulmonary infections, persistent productive cough or hemoptysis. The radiographic manifestations of bronchiectasis have been well studied. They include loss of clarity of vascular markings in specific lung segments, bronchial wall thickening and in advanced bronchiectasis, distinct cystic masses, frequently demonstrating air-fluid levels.[41]

Bronchiectasis is classically described as "cylindrical, varicose, or cystic" based on appearance and other various terms have also been used **(Fig. 32)**. "Tram-tracks" are dilated airways coursing the scan plane. "Signet rings" describe cross-sectional dilated airways with adjacent pulmonary blood artery branches. "Beading airways" are saccular airways seen along their length. There are direct and indirect methods of diagnosing bronchiectasis on CT. Direct methods include bronchial dilatation, lack of normal bronchial tapering, and presence of airways in the periphery of the lungs. Indirect signs consist of bronchial wall thickening and irregularity and the presence of mucoid impaction within the airways.[41]

Bronchiolar Diseases

The introduction of HRCT on assessing small airway disease has significantly impacted the diagnosis and classification of bronchiolar disease.[42] Normal intralobular structures are beyond the resolution of CT; however, direct and indirect signs of bronchiolar disease may be apparent **(Table 4)**.[43] Direct signs include bronchiolar secretions, distinguished as branching Y-shaped linear densities, peribronchiolar inflammation, characterized by poorly defined centrilobular nodules or bronchiolar wall thickening represented by focal small centrilobular lucencies. Indirect signs manifest as either areas of mosaic attenuation on inspiration or as areas of decreased attenuation on expiration.[44] Bronchiolar disease may be categorized on CT into four groups based on other associated signs.

Tree-in-Bud and Bronchiolar Disease

The characteristic finding in this category of bronchiolar disease is the finding of dilated, mucus-filled bronchioles which result in a pattern of centrilobular nodular, branching or Y-shaped densities which imitate the appearance of a tree-in-bud.[45] This pattern is typically seen in infectious bronchiolitis of several etiologies such as bacterial, viral and fungal causes. Common infections resulting in the tree-in-bud representation include *Mycobacterium tuberculosis* infections, atypical mycobacterial infections, bacterial infections related to immunosuppressive conditions, such as HIV and cystic fibrosis.[44] It was initially described in patients with panbronchiolitis,[46] common in Asia. These patients have clinical symptoms of productive cough and dyspnea, with an obstructive impairment on pulmonary physiologic testing and characteristic ill-defined nodules and tree-in-bud appearance on CT. Other proximal airway infection may also depict the tree-in-bud sign in association with other findings. Examples include cystic fibrosis, tuberculosis, postinfectious bronchiectasis and allergic bronchopulmonary mycoses.[47]

Table 4 Conditions associated with bronchiectasis

Disorders	*Description*
Focal distribution	
Bronchial obstruction	Foreign body Tumor Broncholithiasis Compression by peribronchial lymph nodes
Previous pneumonia	
Diffuse distribution	
CF	
Reduced host immunity	Congenital and acquired hypogammaglobulinemia (especially IgG and/or IgG subclasses) HIV infection
Primary ciliary dyskinesia Allergic bronchopulmonary mycoses Chronic MAC infection Aspiration or toxic inhalation Rheumatoid arthritis Inflammation bowel disease	
Other congenital disorders	α_1-antitrypsin deficiency Tracheobronchomegaly (Mounier-Kuhn syndrome) Cartilage deficiency (Williams-Campbell syndrome) Young syndrome Pulmonary sequestration Marfan syndrome
Yellow nail syndrome	

Source: Rosen M. Chronic cough due to bronchiectasis ACCP evidence-based clinical practice guidelines. Chest. 2006;129:122S-31S.

Flow chart 1 summarizes disorders associated with tree-in-bud opacities with individual characteristic features.[43]

Poorly Defined Centrilobular Nodules and Bronchiolar Disease

As compared to infectious bronchiolitis, the distinguishing finding of this group of bronchiolar disease is the presence of ill-defined centrilobular nodules in the absence of a tree-in-bud picture. A variety of diseases with peribronchiolar inflammation without the tree-in-bud patterns have been described. This includes subacute hypersensitivity pneumonitis, lymphocytic interstitial pneumonitis, follicular bronchiolitis, respiratory bronchiolitis-interstitial lung disease and mineral dust-induced bronchiolitis.[44]

Focal Ground Glass Attenuation or Consolidation and Bronchiolar Disease

This presentation of focal ground glass attenuation is the main characteristic of cryptogenic organizing pneumonia (COP) or bronchiolitis obliterans with organizing pneumonia (BOOP).[48] Patients usually complain of symptoms of nonproductive cough for several months, low-grade fever and increasing dyspnea. The most common radiologic finding on HRCT in COP is patchy bilateral consolidation commonly with peribronchial and subpleural distribution.[49] Small, poorly formed peribronchiolar nodules and irregular linear opacities are seen in a smaller percentage of patients. However, the tree-in-bud pattern is clearly uncommon. Areas of ground glass consolidation may be seen in immunocompromised patients with COP.

Flow chart 1 HRCT signs of bronchiolar disorders[43]

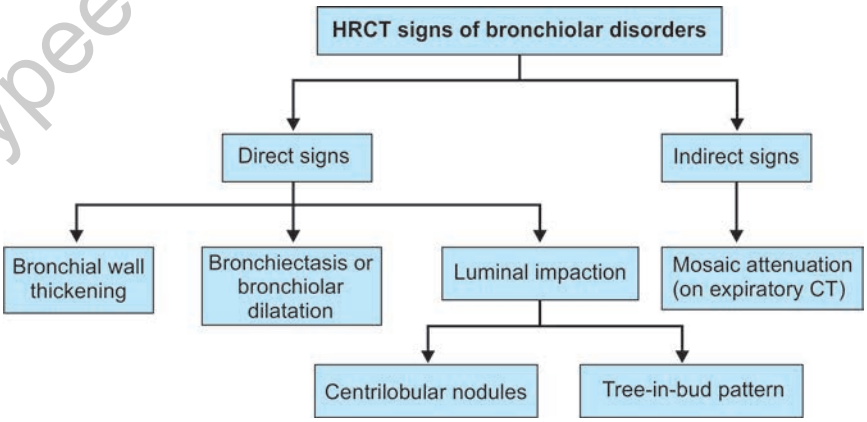

Source: Devakonda A, Raoof S, Sung A, et al. Bronchiolar disorders. A clinical-radiological diagnostic algorithm. Chest. 2010;137:938-51.

Table 5 Characteristic features of bronchiolar diseases with tree-in-bud opacities[43]

	Characteristic clinical features	*Causes and/ or associated conditions*	*HRCT features*	*Histopathologic features*
Infection	Wheezing with concomitant signs of respiratory tract infection	Viral, bacterial, parasitic, mycobacterial, fungal	Tree-in-bud pattern, centrilobular nodules, dense consolidation	Acute and chronic inflammation of small bronchioles with epithelial necrosis and sloughing
Immunologic disorders (allergic bronchopulmonary aspergillosis)	Cough, fever, wheezing; recurrent episodes of bronchial obstruction	Asthma	Tree-in-bud pattern, central bronchiectasis, mucoid impaction, upper lobe predominance	Mucoid impaction of bronchi, eosinophilic infiltration, bronchocentric granulomatosis
Congenital disorders (CF, dyskinetic cilia syndrome)	Recurrent purulent cough, airway hyperactivity	Genetic predisposition, multisystem disease	Tree-in-bud pattern, bronchial wall thickening, bronchiectasis, bronchiolectasis	Cellular infiltration
Neoplasms	Symptoms and signs of upper respirtory tract obstruction (hoarseness, stridor)	Juvenile laryngotracheo-bronchial papillomatosis	Tree-in-bud pattern, multiple solid or cystic nodules	Varies from multiple clusters of squamous cells within alveoli to large cavitary lesions
Diffuse aspiration bronchiolitis	Nonspecific	Elderly, bed bound	Tree-in-bud pattern, centrilobular nodules	Foreign body giant cell reaction
Idiopathic diffuse panbronchiolitis	Mainly in Japanese adults; subacute onset of cough, dyspnea	Associated sinusitis, HLABw54 antigen	Tree-in-bud pattern, thickened ecstatic bronchi, centrilobular nodules	Infiltration of lymphocytes, plasma cells and foamy macrophages at the level of respiratory bronchiole

Abbreviations: CF, cystic fibrosis; HRCT, high-resolution CT
Source: Devakonda A, Raoof S, Sung A, Travis WD, Naidich D. Bronchiolar disorders. A clinical-radiological diagnostic algorithm. Chest. 2010;137:938-51.

Decreased Parenchymal Attenuation and Bronchiolar Disease

This category includes patients with constrictive or obstructive bronchiolitis. Conditions associated with obstructive bronchiolitis include lung transplant, chronic graft-versus-host disease from allogeneic bone marrow transplant and collagen vascular disease.[50] Clinical symptoms are usually mild but severe respiratory compromise may result from progressive airway obstruction. Mosaic attenuation is commonly seen in obstructive bronchiolitis with the presence of bronchial dilatation, peribronchial thickening and evidence of air trapping on expiratory HRCT.[51]

Bronchiolar disease should be approached using systematic method as illustrated in **Table 5**.[43]

PARENCHYMAL DISEASES

Solitary Pulmonary Nodule

The evaluation of focal lung disease in patients poses an imperative challenge in the diagnosis of pulmonary disorders. There is lack of consensus leading to several controversies in the definition, assessment and diagnostic techniques including imaging and mode of pathologic confirmation of focal lung diseases. For the purpose of this chapter, we will define an SPN as a single, rounded lesion in the lung parenchyma, which is not associated with atelectasis or pneumonia. The SPNs are a common, incidental finding on CT imaging. Characterization of the pulmonary nodule is of utmost importance and may aid in narrowing the differential diagnosis, preventing unnecessary procedures or missing localized malignancy. The differential diagnosis of SPNs is depicted in **Flow chart 2**.[52]

Size

The size of an SPN on CT has been shown to directly influence the probability of malignancy.[53] Nodules larger than 3 cm are more apt to being malignant. However, smaller lesions, even of less than 1 cm in size, have been shown to be malignant in several studies.[54]

Location

Primary lung cancers have been shown to be more commonly located in the upper lobes, particularly on the right side.[55] The SPNs have also been reported to be identified in the lung

Flow chart 2 A stepwise approach to bronchiolar disease.[43] History, physical findings, evidence of hyperinflation on chest radiograph or airflow obstruction on pulmonary function testing suggestive of bronchiolar disease, should trigger a request for obtaining an HRCT scan of the chest performed at the end of inspiration and expiration. An HRCT scan of the chest further classifies bronchiolar diseases. The presence of a tree-in-bud pattern largely suggests either an infectious bronchiolitis, if a focal distribution is noted, or diffuse panbronchiolitis or congenital disease related bronchiolitis, if a diffuse pattern is noted. If centrilobular nodules are predominantly seen, then RB-ILD should be suspected in a smoker or HP in a non-smoker. Mosaic attenuation suggests either a constrictive bronchiolitis or obliterative bronchiolitis. Histology is ultimately required for the final confirmation

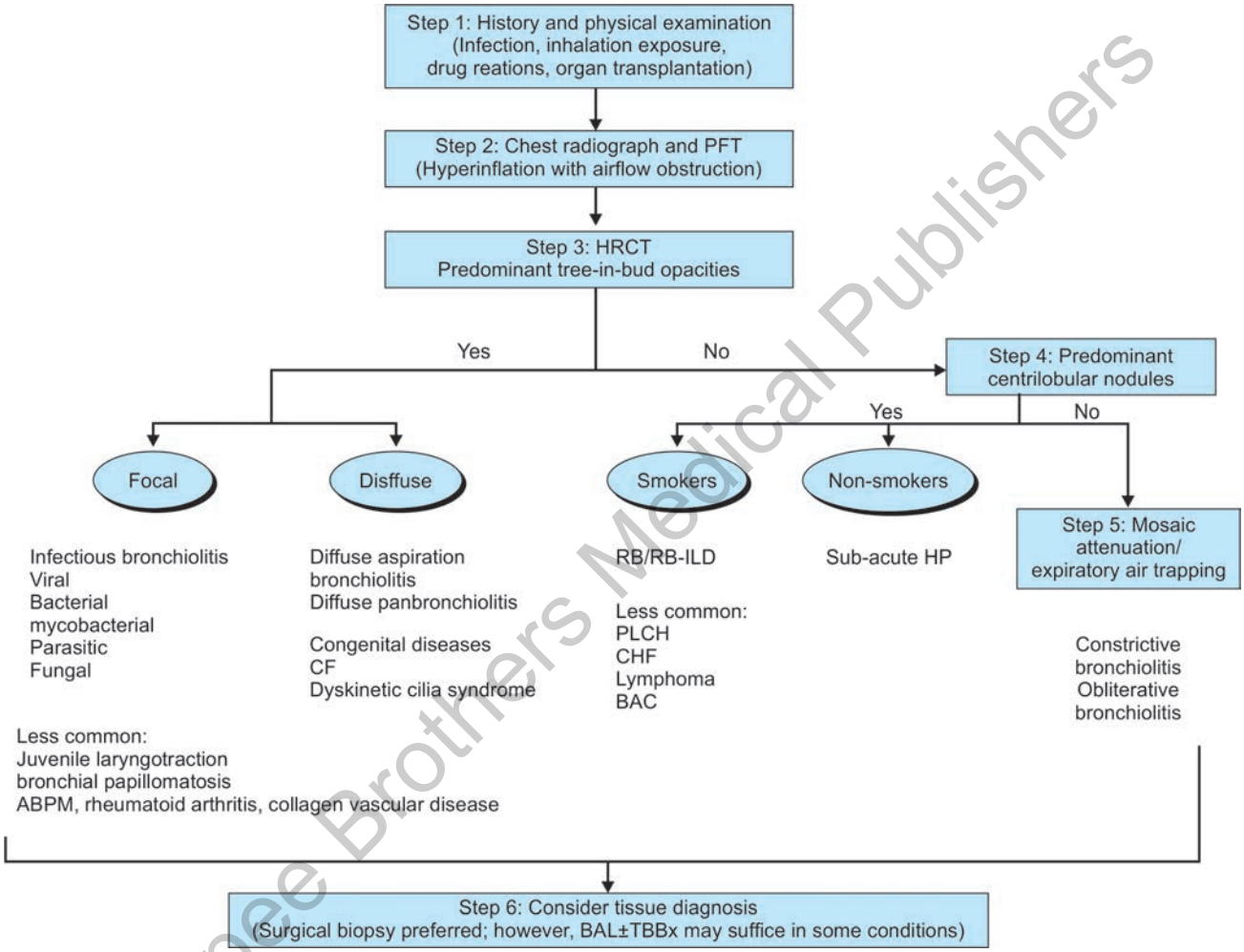

Abbreviations: ABPM, allergic bronchopulmonary mycosis; BAC, bronchoalveolar cell carcinoma; CF, cystic fibrosis; CHF, congestive heart failure; HP, hypersensitivity pneumonitis; PFT, pulmonary function test; PLCH, pulmonary Langerhans cell histiocytosis; RB-ILD, respiratory bronchiolitis-inetrstitial lung disease; TBBx, transbronchial biopsy

Source: Devakonda A, Raoof S, Sung A, Travis WD, Naidich D. Bronchiolar disorders. A clinical-radiological diagnostic algorithm. Chest. 2010;137:938-51.

periphery, rather than the medial third of the lung. Metastatic lesions are predisposed to be subpleural in location, predominantly seen in the lower lobes.[56] Nevertheless, several other lesions, such as lymph nodes, are also seen in the subpleural distribution.[57]

Margin and Contour

Benign nodules tend to demonstrate a round, smooth contour with a sharply defined margin. Malignant lesions are more likely to exhibit an irregular lobulated or ragged shape and

a vague, irregular, or spiculated edge.[58] Malignant lesions have been reported to demonstrate a smooth appearance and benign conditions have shown lobulated or spiculated contours.[59] **Table 6** illustrates margin characteristics in benign and malignant processes.[52]

Halo Sign

A halo sign is defined as a distinct nodule surrounded by a circular margin of ground glass attenuation.[60] This sign has been most commonly associated with the early course of invasive pulmonary aspergillosis in the correct clinical context. It has also been reported in Wegener's granulomatosis, Kaposi's sarcoma and bronchoalveolar carcinoma.

Bronchus Sign

The identification of an air bronchogram on CT is of important value. Although nonspecific, the presence of bronchial lumen surrounded by a pulmonary lesion is likely to be malignant. Airways related to lung cancer tend to be abnormal, appearing ecstatic or tortuous.[61]

Cavitation

Several etiologies may result in cysts and cavities, including septic emboli, vasculities and tumors. CT helps in characterizing cysts and cavities, allowing for closer evaluation of wall thickness and intracavitary findings such as air-fluid levels. Thin-walled cavities tend to be benign and thick-walled cavities of uncertain etiology.[62]

Feeding Vessel Sign

A focal lesion with an adjacent vessel is known as a feeding vessel sign or vessel-mass sign, has been described in various conditions such as arteriovenous malformations, metastasis or infarcts.[63] Although, not reported to be a common finding, a feeding vessel sign is helpful in distinguishing hematogenous metastasis from either primary or granulomatous lesions. It is also useful in diagnosing septic emboli and pulmonary vasculitis in the appropriate clinical situation.

Growth Rates

One of the most important radiographic factors allowing for distinction between benign and malignant disease is the growth rate of the SPN. It is, therefore, paramount to review prior chest images in the evaluation of an SPN. The absence of detectable growth over a 2-year period is highly suggestive of a benign etiology.[64] The doubling time for an SPN is the time it takes to double in size which can be determined using the changes in diameter. A 26% increase in diameter will result in a doubling volume of an SPN. A majority of malignant SPNs have a doubling time of 20–400 days.

Table 6 Differential diagnosis of solitary pulmonary nodules[52]

Infections
Tuberculosis (TB)
Round pneumonia, organizing pneumonia
Lung abscess
Fungal: aspergillosis, blastomycosis, cryptococcosis, histoplasmosis, coccidioidomycosis
Parasitic amoebiasis, echinococcosis, Dirofilaria immitis (Dog heartworm)
Measles
Nocardia
Atypical mycobacteria
Pneumocystis jiroveci
Septic embolus
Neoplastic
Benign
Hamartoma
Chondroma
Fibroma
Lipoma
Neural tumor (Schwannomna neurofibroma)
Sclerosing hemangioma
Plasma cell granuloma
Endometriosis
Malignant
Lung cancer
Primary pulmonary carcinoid
Solitary metastasis
Teratoma
Leiomyoma
Vascular
Arteriovenous malformation
Pulmonary infarct
Pulmonary artery aneurysm
Pulmonary venous varix
Hematoma
Congenital
Bronchogenic cyst
Lung sequestration
Bronchial atresia with mucoid impaction
Inflammatory
Rheumatoid arthritis
Granulomatosis with polyangiitis (Wegener)
Microscopic polyangiitis
Sarcoidosis
Lymphatic
Intrapulmonary lymph node
Lymphoma
Outside lung fields
Skin nodule
Nipple shadows
Rib fracture
Pleural thickening, mass or fluid [pseudotumor, (i.e. loculated fluid)]
Miscellaneous
Rounded atelectasis
Lipoid pneumonia
Amyloidosis
Mucoid impaction (mucocele)
Infected bulla
Pulmonary scar

Source: Patel VK, Naik SK, Naidich DP, Travis WD, Weingarten JA, Lazzaro R, et al. A practical algorithm approach to the diagnosis and management of solitary pulmonary nodules: part 1: radiologic characteristics and imaging modalities. Chest. 2013;143(3):825-39.

Table 7 Margin characteristics of solitary pulmonary nodules[52]

Margin	*Etiology*
Smooth	Suggests a benign lesion. However, may be malignant in up to one-third of cases[50,51]
Lobulated	Suggests uneven growth; a PPV of 80% for malignancy.[45,46] Up to 25% of benign lesions, such as hamartomas can have lobulated margins
Spiculated	A spiculated margin (the so-called corona radiata sign) is highly predictive of malignancy, with a PPV of 88% to 94%. A few exceptions of benign SPNs that could have spiculated margins include lipoid pneumonia, focal actelectasis, tuberculoma, and progressive massive fibrosis[45,54]
Ragged	Suggests growth pattern along the alveolar wall; lepidic pattern of adenocarcinoma
Tentacle or polygonal	Seen in fibrosis, alveolar infiltration, and collapsed alveoli
Halo	SPN surrounded by a "halo" of ground glass attenuation, also called the " CT halo sign". Seen in aspergillosis, Kaposi sarcoma, granulomatosis with polyangiitis (Wegener), and metastatic angiosarcoma. Adenosarcoma in situ (previously known as bronchoalveolar carcinoma) can also produce a halo due to its lepidic growth
Notches	SPN with notches or concavity in the margin is seen in some SPNs with tumor growth. These notches are frequently found in adenocarcinomas with overt invasion and are associated with poor prognosis[17]
Source: Patel VK, Naik SK, Naidich DP, Travis WD, Weingarten JA, Lazzaro R, et al. A practical algorithm approach to the diagnosis and management of solitary pulmonary nodules: part 1: radiologic characteristics and imaging modalities. Chest. 2013;143(3):825-39.	

Calcification

The radiographic presence of calcification can suggest that a pulmonary lesion is benign.[65] Four patterns of benign calcification have been studied: (1) laminated and concentric; (2) dense central core; (3) diffuse and solid; and (4) punctuate. There is no specific pattern of calcification associated with malignant nodules. Calcification classically appears speckled or eccentric and usually within large central lesions.[66] Refer to **Table 7** for patterns of calcifications in benign and malignant processes.[52]

Fat

The appearance of fat is suggestive of two key conditions: hamartoma or exogenous lipoid pneumonia. A hamartoma is a benign condition which contains connective tissue, cartilage, smooth muscle, bone and variable amounts of fat and represents the third most common cause of an SPN.[67] They can be diagnosed by CT as lesions containing fat or fat and calcification have an even contour with a sharp circumference.

Contrast Enhancement

Due to the fundamental differences in vascularity of focal benign versus malignant lesions, the phenomenon of pulmonary enhancement has been a valuable tool in differentiating the two processes.[68] Malignant lesions are more prone to enhancement following injection of contrast material. It has been reported that malignant lesion may enhance by greater than 15–20 Hounsfield units.[69]

Diffuse Diseases

Diffuse parenchymal lung diseases include chronic and acute infiltrative lung diseases and emphysema. These conditions, in addition to being diffuse in nature, often have patchy or focal distribution. Suggestive findings that indicate parenchymal irregularity in diffuse lung disease include linear and reticular opacities, nodular opacities, and increased attenuation seen as consolidation or ground glass opacities and decreased attenuation seen in emphysema and cystic diseases.

Several acute and chronic pulmonary conditions result in diffuse infiltration of the lungs. They can be classified based on the predominant radiographic pattern on CT **(Table 8)**.[70] There are seven distinct histologic types of idiopathic interstitial pneumonias: (1) Usual interstitial pneumonia/idiopathic pulmonary fibrosis (UIP/IPF), (2) nonspecific interstitial pneumonia (NSIP), (3) desquamative interstitial pneumonia (DIP), (4) respiratory bronchiolitis interstitial pneumonia (RBILD), (5) acute interstitial pneumonia (AIP), (6) cryptogenic organizing pneumonia/bronchiolitis obliterans organizing pneumonia (COP/BOOP) and (7) lymphocytic interstitial pneumonia (LIP).[71] HRCT evaluation may avoid the necessity for tissue diagnosis and may limit the differential diagnosis in some cases.

Reticular Pattern

Idiopathic pulmonary fibrosis: Idiopathic pulmonary fibrosis has characteristic HRCT findings that can lead to its diagnosis with a high degree of certainty.[72] In the early phase of IPF, patchy peripheral distribution of ground glass opacities is seen with areas of normal lung intermingled in between.

Table 8 Patterns of calcifications in solitary pulmonary nodules[52]

Patterns of calcification	*Etiology*
Laminated and concentric	Usually benign
Dense central core	Usually benign
Diffuse and solid	Usually benign
Popcorn	Hemartoma
Punctate	Malignant lesions: scar carcinoma, typical and atypical carcinoids large-cell neuroendocrine carcinoma and metastasis from colon, ovary, breast, thyroid, and osteogenic tumors
Eccentric	Due to necrosis within the malignant nodule or engulfment of adjacent granuloma
Source: Patel VK, Naik SK, Naidich DP, Travis WD, Weingarten JA, Lazzaro R, et al. A practical algorithm approach to the diagnosis and management of solitary pulmonary nodules: part 1: radiologic characteristics and imaging modalities. Chest. 2013;143(3):825-39.	

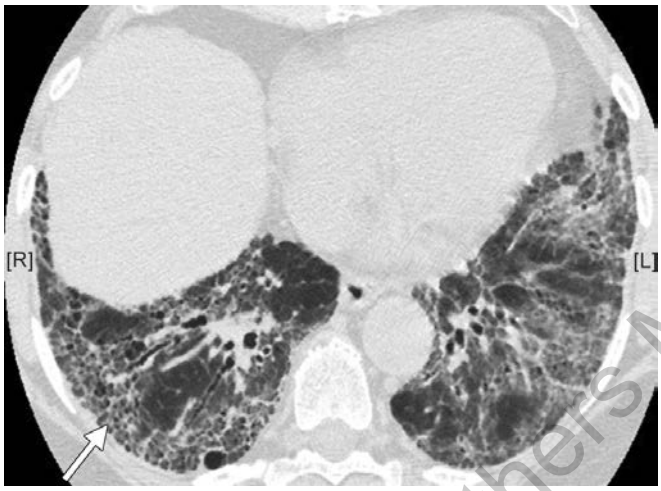

Fig. 33 HRCT showing cuts through the lower lobes showing reticular changes including honeycombing, traction bronchiectasis and architectural distortion

Fig. 34 CT chest features of nonspecific interstitial pneumonia (NSIP) with diffuse, bilateral ground glass attenuation at the lower lung zones. Note the absence of honeycombing

The main pattern of abnormality seen on HRCT in a later stage in patients with IPF include intralobular linear opacities, which correspond to histologic areas of fibrosis, a fine reticular pattern, most pronounced at the lung bases and in the subpleural regions and irregular interfaces between the lung and pulmonary vessels, bronchi and pleural surfaces[73] **(Fig. 33)**. This progression of fibrosis ultimately results in dilatation and tortuosity of bronchi and bronchioles, referred to as traction bronchiectasis. The end stage of IPF is illustrated by honeycombing, noted most severely at the lung bases and in subpleural sites.[74] The IPF is classically represented as a patchy distributed disease, with spatial and temporal heterogeneity. This refers to areas of normal lung, reticular changes or honeycombing seen in the same patient within the same lung section.

Nonspecific interstitial pneumonitis: There are two forms of nonspecific interstitial pneumonia (NSIP) which can occur: "cellular or a fibrotic NSIP". HRCT features of NSIP include ground-glass attenuation in a diffuse or patchy distribution with reticular opacities and traction bronchiectasis.[75] In cellular NSIP, there is prevalence of ground-glass attenuation **(Fig. 34)** and in fibrotic NSIP more reticular changes are noticeable **(Fig. 35)**. Findings of honeycombing are seldom noted. NSIP, unlike UIP, displays temporal and spatial homogeneity, where there is a uniform pattern of HRCT changes within the same lung segment.

Collagen vascular disease: High-resolution CT features similar to IPF may be seen in various collagen vascular diseases such as rheumatoid arthritis, scleroderma, mixed connective tissue disease, polymyositis and systemic lupus erythematosis.[76] Rheumatoid arthritis may result in fibrosis in a small percentage of patients, with a similar lower lung zone distribution as IPF. More commonly seen are pleural manifestations but other findings, such as bronchiectasis or

Fig. 35 CT chest through the middle lung zones in a patient with nonspecific interstitial pneumonia (NSIP)

rheumatoid nodules can occur.[77] Scleroderma may result in fibrosis with fine reticulation as well as ground-glass attenuation, honeycombing or pleural thickening.[78]

Asbestosis: Asbestosis leads to predominantly basilar and dorsal lung parenchymal fibrosis. Other characteristic findings include: peribronchiolar fibrosis that forms centrilobular nodules, intralobular and interlobular septal fibrosis that forms subpleural short lines, coarse parenchymal bands, and subpleural curvilinear bands that parallel the pleura and represent fibrotic bridging from one centrilobular region to the next.[79] Coarse honeycombing can be seen in advanced stages. Coexistent pleural plaques are frequently identified, particularly in patients with curvilinear subpleural lines.[80]

Nodular Pattern

The differential diagnosis of nodular disease includes an extensive list of benign and malignant processes. Nodular disease can be further analyzed based on the predominant distribution of nodules: perilymphatic; centrilobular; or random[11] **(Table 9)**.

Perilymphatic Distribution

Sarcoidosis: The characteristic HRCT finding of sarcoidosis includes small nodules and nodular thickening along the bronchovascular bundles, interlobular septa, interlobular fissures, and subpleural lung regions[81] **(Figs 36 and 37)**. The bronchovascular thickening is most pronounced at the hila. The nodules appear irregular and represent coalescence of microscopic granulomas. The "galaxy sign" is a term used to describe an irregularly marginated pulmonary nodule formed by a confluence of multiple smaller nodules. The concentration of smaller nodules becomes less dense towards the periphery resulting in irregular borders and multiple satellite nodules, resembling the appearance of a galaxy.[82] As fibrosis develops, reticular changes, such as intralobular septal thickening occur which ultimately lead to architectural distortion, loss of lung volume and traction bronchiectasis.[83] Honeycombing may also be seen, although it is usually mild

Table 9 Radiographic patterns of diffuse lung disease

Pattern of opacities	*Acute*	*Chronic*
Consolidation	Infection, acute respiratory distress syndrome, hemorrhage, aspiration, acute eosinophilic pneumonia, acute interstitial pneumonia, cryptogenic organizing pneumonia	Chronic infections (tuberculosis, fungal), chronic eosinophilic pneumonia, cryptogenic organizing pneumonia, lymphoproliferative diseases, bronchioloalveolar carcinoma, pulmonary alveolar proteinosis and sarcoidosis
Linear or reticular opacities	Infections (viral, mycoplasma), pulmonary edema	Idiopathic pulmonary fibrosis or usual interstitial pneumonia, connective tissue disease–associated pulmonary fibrosis, asbestosis, sarcoidosis, hypersensitivity pneumonitis, drug-induced lung disease
Small nodules	Infections (disseminated tuberculosis, fungal or viral infections), hypersensitivity pneumonitis	Sarcoidosis, hypersensitivity pneumonitis, silicosis,coal worker's pneumoconiosis, respiratory bronchiolitis, metastases, alveolar microlithiasis
Cystic airspaces	*Pneumocystis carinii* pneumonia, septic embolism	Pulmonary Langerhans cell histiocytosis, pulmonary lymphangioleiomyomatosis, honeycomb lung, metastatic disease
Ground-glass opacities	Infections (*P. carinii*, cytomegalovirus), pulmonary edema, hemorrhage, hypersensitivity pneumonitis, acute inhalational exposures, drug-induced lung diseases, acute interstitial pneumonia	Nonspecific interstitial pneumonia, respiratory bronchiolitis–associated interstitial lung disease, desquamative interstitial pneumonia, drug-induced lung diseases, pulmonary alveolar proteinosis
Thickened interlobular septa	Pulmonary edema	Lymphangitic carcinomatosis, pulmonary alveolar proteinosis, sarcoidosis, pulmonary veno-occlusive disease

Fig. 36 HRCT at the level of the right upper lobe bronchus showing small nodules and nodular thickening along the bronchovascular bundles, interlobular septa, interlobular fissures, and subpleural lung regions in a patient with sarcoidosis

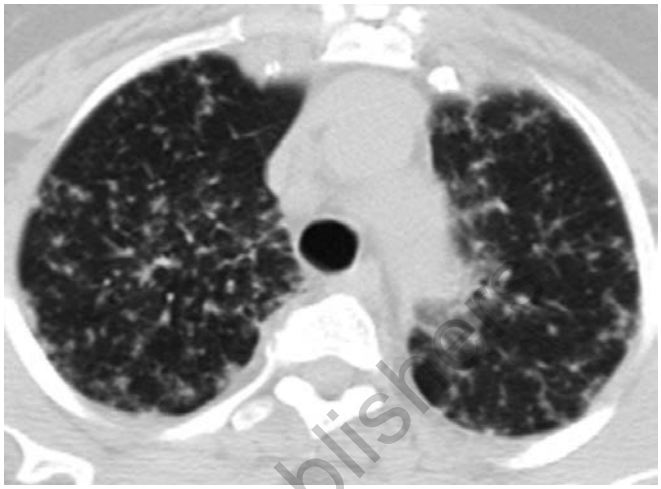

Fig. 37 HRCT through the upper lung zones showing multiple small nodules throughout with nodules seen along the subpleural regions and along the interlobular septa and interlobular fissures

and involves primarily the upper and middle lung zones, with relative sparing of lung bases.[84] Hilar and mediastinal lymphadenopathy is another feature of sarcoidosis seen on CT, with calcification noted in long-standing disease.[85]

Silicosis/Coal Workers Pneumoconiosis: The most characteristic findings in silicosis and coal worker's pneumoconiosis are small nodules predominantly seen in the posterior aspects of the upper lung zones. These nodules vary in size, may be calcified and are distributed largely in the centrilobular pattern.[86] Progressive massive fibrosis is seen as a conglomerate of nodules with an irregular margin, often resulting in architectural distortion.

Lymphangitic carcinomatosis: Pulmonary lymphangitic carcinomatosis refers to lymphangitic or hematogenous spread of tumor to the lungs resulting in infiltration and thickening of the interlobular septa, subpleural interstitium, and bronchovascular bundles and preservation of the normal lung architecture **(Fig. 38)**.[87] The thickening of these structures may be smooth or have a nodular appearance, may be diffuse and bilateral or focal and unilateral in distribution **(Fig. 39)**. The most common primary malignancies resulting in lymphangitic carcinomatosis are adenocarcinoma of the breast, lung, gastrointestinal tract and prostate.

Fig. 38 HRCT through upper lobes demonstrating intralobar septal thickening in a patient with lymphangitis carcinomatosis

Centrilobular Distribution (Ground-Glass Nodules)

Hypersensitivity pneumonitis: Hypersensitivity pneumonitis, also known as extrinsic alveolitis represents a type 3 allergic reaction or immune complex disease. HRCT is most useful in diagnosing subacute hypersensitivity pneumonitis, where it displays diffuse or patchy ground-glass opacification with lobular sparing, lobular air-trapping, and centrilobular poorly defined airspace nodules.[88] The ground-glass attenuation is noted predominantly in the middle and lower lung zones and may be present in combination with mosaic attenuation **(Fig. 40)**. In chronic hypersensitivity pneumonitis, fibrosis, represented by a reticular pattern, architectural distortion and ultimately honeycombing are seen with relative basilar sparing.[89]

Lymphocytic interstitial pneumonitis: Lymphocytic interstitial pneumonitis can be seen in patients with Sjögren's syndrome and is seen commonly in children with acquired immune deficiency syndrome. Dense infiltration of monoclonal or polyclonal T lymphocytes occurs in the interstitium. It can

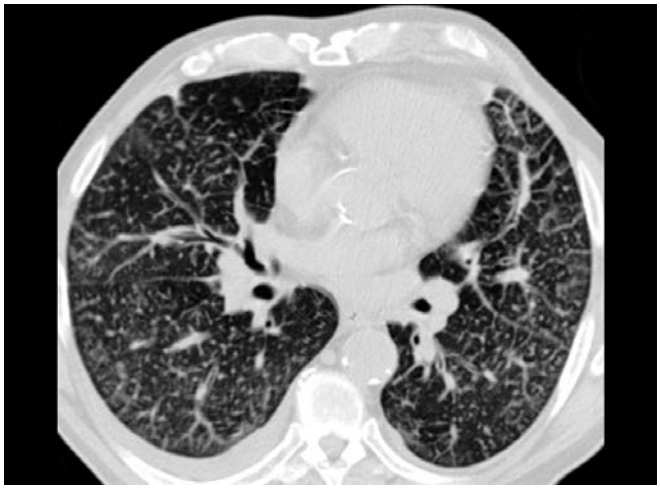

Fig. 39 HRCT at the level of the lower lobe bronchi showing a fine reticular pattern from interlobular septal thickening and multiple tiny nodules in a patient with lymphangitic carcinomatosis. Note the extension of the irregular interlobular septal thickening to the pleural surface

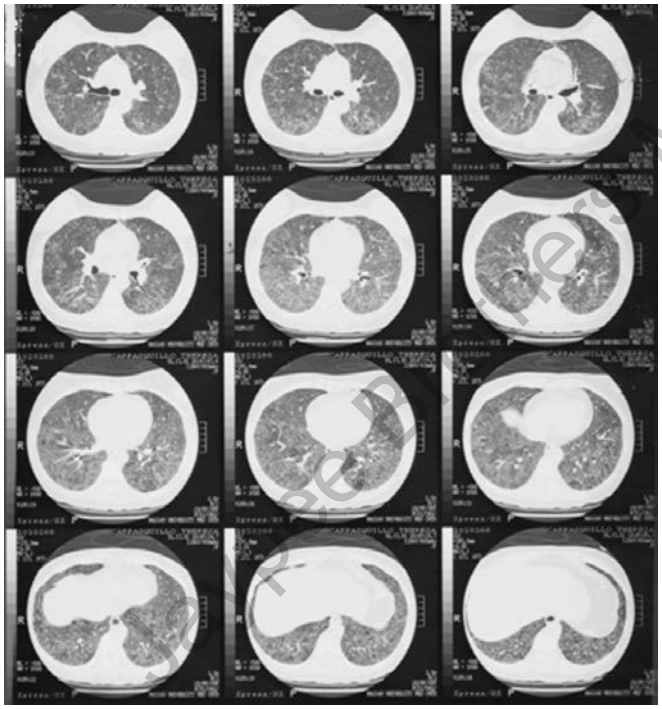

Fig. 40 CT chest representing hypersensitivity pneumonitis. Numerous centrilobular nodules which are poorly defined and shown to extend to the periphery are illustrated

lead to lymphoma of the lung parenchyma. The characteristic features on HRCT include ground-glass opacities, reticular opacities and perivascular cysts **(Figs 41 and 42)**.[90]

Fig. 41 CT chest through the upper lobes demonstrating cystic changes in a patient with LIP. Also noted is a pleural effusion on the right

Fig. 42 CT chest through the lower lungs demonstrating cystic changes in a patient with lymphocytic interstitial pneumonitis
Courtesy: Dr A Saleh

Centrilobular Distribution (Tree-in-Bud)

Panbronchiolitis: Panbronchiolitis is a form of diffuse bronchiolitis reported in Asia, especially from Japan and Korea.[91] The characteristic CT features of diffuse tree-in-bud pattern are seen mainly affecting the lower lung zones, with complete resolution after macrolide therapy. Typically seen are centrilobular nodular and linear opacities corresponding to thickened and dilated bronchiolar walls with intraluminal mucous plugs, mosaic attenuation, peripheral air trapping and bronchiectasis, especially in advanced disease.[92]

Infectious etiology: The tree-in-bud pattern is frequently seen in several airway infections of bacterial and viral etiologies;

tuberculosis, *Mycobacterium avium* intracellulare and fungal infections such as allergic bronchopulmonary mycosis (ABPM).[48]

Random Distribution

Hematogenous metastasis: Hematogenous tumor metastasis most commonly results in localized tumor nodules, rather than lymphatic infiltration. Multiple, large, well-defined nodules involving the lower lung zones are seen in a randomly distributed fashion.[93]

Pulmonary Opacities

Ground-Glass Opacities:

Desquamative interstitial pneumonitis/respiratory bronchiolitis interstitial lung disease: Desquamative interstitial pneumonitis (DIP) and respiratory bronchiolitis interstitial lung disease are related disorders exclusively found in smokers. The major HRCT finding in patients with respiratory bronchiolitis is the presence of ill-defined, centrilobular ground-glass nodules, primarily in the upper lobes. DIP may be distinguished from RB-ILD by the presence of ground-glass attenuation, which is predominantly found in the middle and lower lung zones[94] **(Fig. 43)**. Mild fibrosis indicated by irregular linear opacities, architectural distortion and honeycombing may be seen in the subpleural and lower lung regions.

Acute interstitial pneumonitis: Acute interstitial pneumonitis, also known as Hamman-Rich syndrome, is characterized by an acute onset and rapid progression. HRCT findings are of diffuse ground-glass attenuation and consolidation with abnormalities suggestive of fibrosis, such as traction bronchiectasis.[95]

Pulmonary alveolar proteinosis: Pulmonary alveolar proteinosis (PAP) results from ineffective clearance of surfactant from alveoli. The predominant HRCT features of PAP consist of bilateral areas of ground-glass opacification with smoothly thickened interlobular septal lines.[96] There may be lobular or geographic sparing. Other features seen on HRCT include poorly defined nodular opacities and consolidation.[97] The "crazy-paving sign" seen with PAP as well as other interstitial lung conditions is a pattern characterized by reticular markings superimposed on ground glass opacities.[98]

Consolidation

Bronchiolitis obliterans with organizing pneumonia/Cryptogenic organizing pneumonia: HRCT typically shows peribronchial and peripheral areas of consolidation **(Figs 44 and 45)**.[99] Another suggestive finding is the presence of rings or crescents of consolidation surrounding ground-glass opacities, which has been called a "reverse halo" sign.[100]

Bronchoalveolar carcinoma: Bronchoalveolar carcinoma may present with three distinct patterns.[101] It may present as a small solitary nodule, which has a characteristic ground-glass appearance on CT, suggestive of a good prognosis. It may also present as lobar consolidation resembling bacterial pneumonia, where the CT features typically show air bronchograms. Sometimes it presents with multifocal pulmonary nodules.

Cystic Diseases

There are many pulmonary conditions that may result in cystic changes on CT. **Flow chart 3** illustrates the classification of multiple hypolucent lesions according to the distributive pattern.

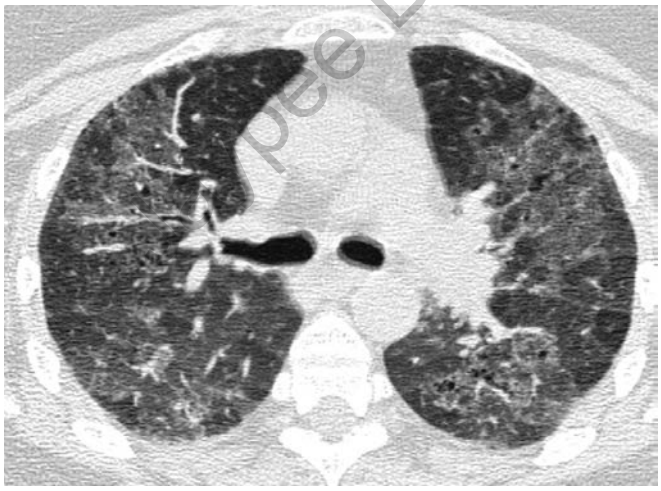

Fig. 43 CT chest through the upper lobes in a patient with desquamative interstitial pneumonitis showing a diffuse ground-glass attenuation

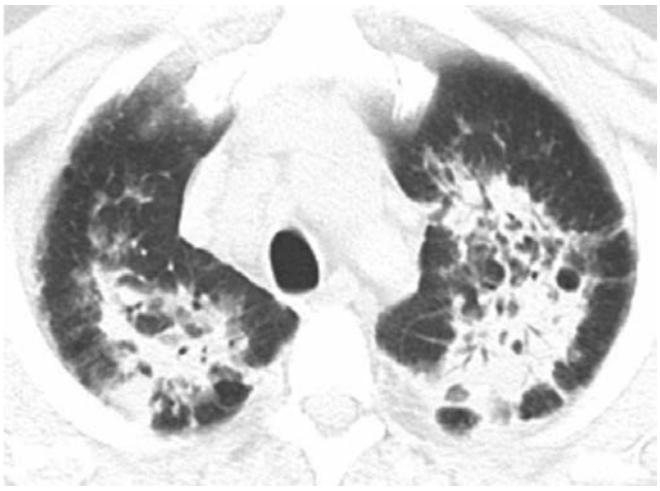

Fig. 44 CT chest showing bilateral dense consolidation in the upper lobes in cryptogenic organizing pneumonia

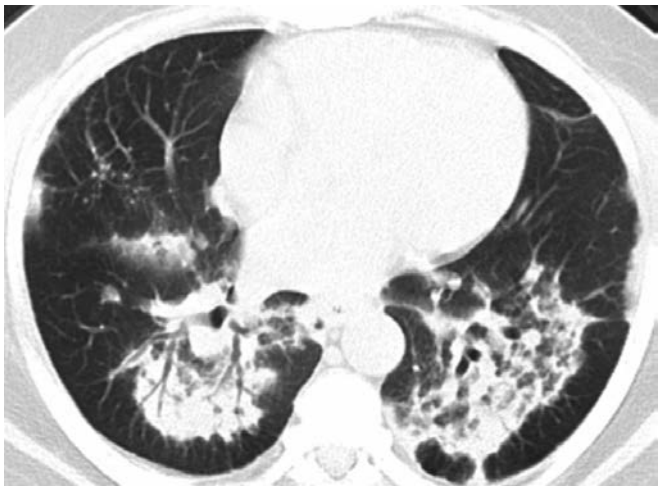

Fig. 45 CT chest through the lung bases showing dense bilateral consolidation with air bronchograms in a patient with cryptogenic organizing pneumonia

Lymphangioleiomyomatosis: Lymphangioleiomyomatosis (LAM) affects women of reproductive age, results from smooth muscle proliferation within the pulmonary interstitium causing thickening of walls of lymphatics, blood vessels and bronchioles. Patients present with spontaneous pneumothorax, chylothorax, hemoptysis and marked hyperexpansion of lungs. Characteristic HRCT features of LAM consist of diffuse thin-walled cysts surrounded by normal lung without regional sparing[102] **(Fig. 46)**. The cysts are rounded, may vary in size but bizarre shaped cysts as those seen in Langerhans cell histiocytosis (LCH) are unlikely[103] **(Fig. 47)**.

Langerhans cell histiocytosis: Langerhans cell histiocytosis also known as eosinophilic granuloma or histiocytosis X is a smoking-related lung disease with 80–100% of cases seen in patients with a history of smoking.[104] It is recognized on CT by the presence of cysts showing an upper lobe predominance, especially in the early stages. The initial changes include

Flow chart 3 Algorithmic approach to multinodular lung disease

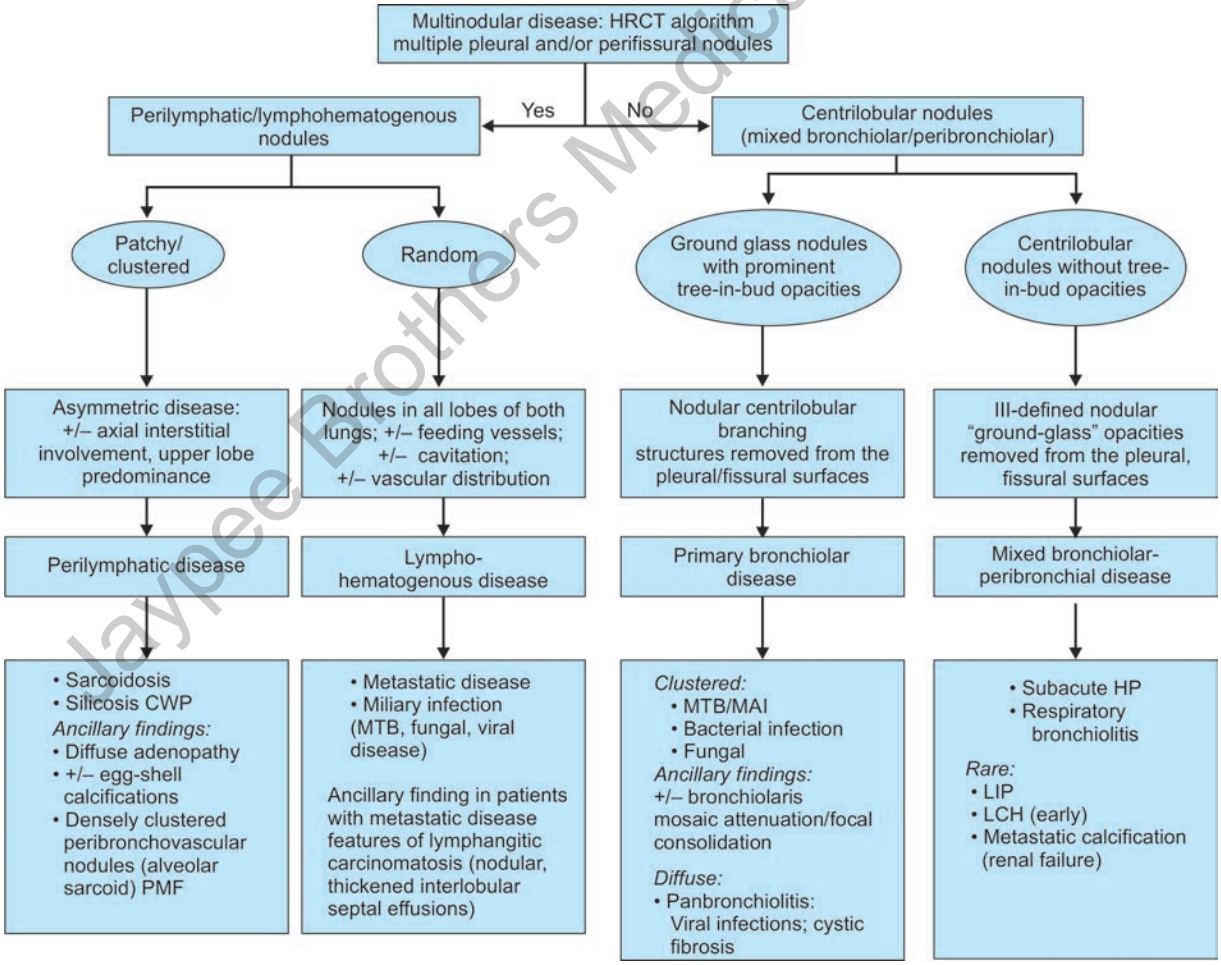

Abbreviations: CWP, coal workers pneumocontosis; MAI, M atrium intracellulare; MTB, M tuberculosis; PMF, progressive massive fibrosis
Source: Raoof S, Amchentsev A, Vlahos I, et al. Pictorial essay: mulitinodular disease: a high-resolution CT scan diagnostic algorithm. Chest. 2006; 129(3):805-15.

Fig. 46 CT chest through the upper lobes showing diffuse cystic changes in a patient with lymphangioleiomyomatosis. The cysts are evenly distributed and have thin, definable walls. Note the absence of nodules

Fig. 47 CT chest in a patient with lymphangioleiomyomatosis showing well-defined, multiple cysts with uniform distribution at the lung bases

Fig. 48 HRCT through the upper lobes in a patient with Langerhans cell histiocytosis. There are nodules present with irregular cysts with thin and thick walls

Fig. 49 A classic CT chest representation of diffuse ground glass attenuation in a patient with *Pneumocystic carinii* pneumonia

small nodular opacities with sharply defined or stellate centrilobular nodules seen on HRCT. Multiple thin-walled cysts of varying size are usually present, scattered throughout the upper and middle lung zones with relative sparing of the bases. The cysts have bizarre, irregular shapes, which can appear in combination with nodules in the intermediate stages of the disease **(Fig. 48)**.[105]

Pneumocystis pneumonia: Pneumocystis jiroveci pneumonia (PJP), previously called *Pneumocystis carinii* pneumonia is one of the most common pulmonary infections in patients with AIDS. The HRCT findings consist of bilateral ground-glass attenuation, which appear consolidated with severe disease and a distinct mosaic pattern with areas of normal lung interspersed between areas of ground-glass opacities[106] **(Figs 49 and 50)**. Other associated findings include pneumothoraces and cystic lung changes **(Figs 51 and 52)**.

MEDIASTINAL DISEASES

The mediastinum is bounded laterally by the lungs, anteriorly by the sternum, and posteriorly by the vertebral bodies. Several focal and diffuse conditions may occur within the mediastinum. The mediastinum can be divided into compartments based on CT landmarks to facilitate the differential diagnosis. These include the anterior mediastinum, which includes the retrosternal clear space and the cardiophrenic angle; the middle mediastinum, which includes the retrosternal clear space, subcarinal region, and retrocardiac clear space; and the posterior mediastinum. It should be pointed out that there are no physical boundaries

Fig. 50 CT chest showing a diffuse ground glass pattern with a crazy paving appearance in a patient with *Pneumocystic carinii* pneumonia

Fig. 52 HRCT through the upper lung zones showing a dense opacity in the right upper lobe, ground glass opacities in the left upper lobe, small and large (arrows) cysts in a patient with *Pneumocystic jiroveci* pneumonia

Fig. 51 CT chest in a patient with *Pneumocystic carinii* pneumonia with evidence of pneumothorax and bilateral diffuse haziness

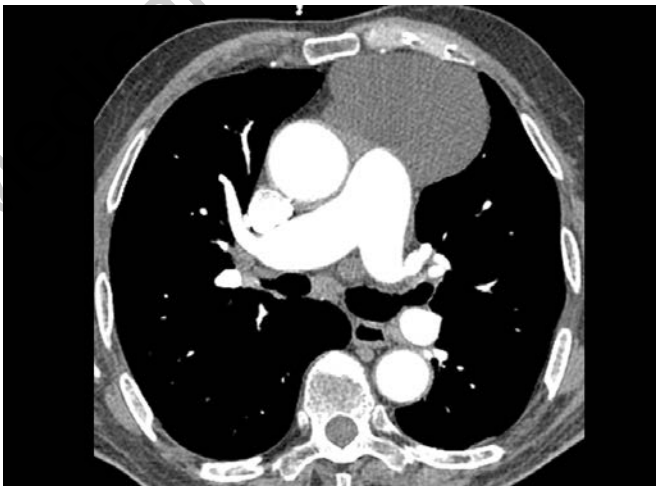

Fig. 53 CT chest (mediastinal window) illustrating a large mediastinal mass in the retrosternal clear space. Note the homogeneous appearance. This is representative of a thymic cyst

between different compartments that may limit any mediastinal disease **(Flow chart 4)**.

Retrosternal Clear Space

This region is bordered anteriorly by the sternum and posteriorly by the aorta and great vessels. The normal structures located in this region include the thymus gland, lymph nodes, and fat. Abnormalities involving the retrosternal clear space include thymoma, thymic cyst, lymphoma, teratoma, aortic aneurysm or lipoma. Thymomas represent a majority of anterior mediastinal lesions in adults. The CT appearance of a thymoma shows a homogeneous soft-tissue rounded or lobulated mass, which is sharply demarcated and does not conform to the normal shape of thymus.[107]

Thymic cysts are thin walled with air fluid levels on CT **(Fig. 53)**. Teratomas are seen with a combination of fluid-filled cysts, fat, soft tissue and calcification.[108]

Cardiophrenic Angle

The cardiophrenic angle is the space anterior to and the right of heart. Usual abnormalities are the benign lesions such as fat, lipoma, pericardial cyst or Morgagni hernia.

Retrotracheal Clear Space

The retrotracheal space includes structures posterior to the trachea, anterior to the thoracic spine and superior to the aortic arch. The normal structures in this area include

Flow chart 4 Multiple lucent lesions are classified according to their distribution pattern as either focal or diffuse. The focal lucencies can further be distinguished into upper lobe, lower lobe or random distribution. Examples of diffuse lucent lesions include panacinar emphysema, LAM, LIP or congenital disease related diffuse bronchiectasis. Examples of focal upper lung lucent lesions include centrilobular or paraseptal emphysema, LCH with presence of small nodules and infectious etiologies. Focal lower lung lucencies are usually seen in interstitial lung diseases such as UIP, DIP and RBILD as cystic changes with ground glass opacities also seen in DIP and RBILD. Randomly distributed focal lucencies may be seen in a braod group of conditions such as rheumatoid arthritis, necrotizing pneumonia and cavitating infarctions after a pulmonary embolism.

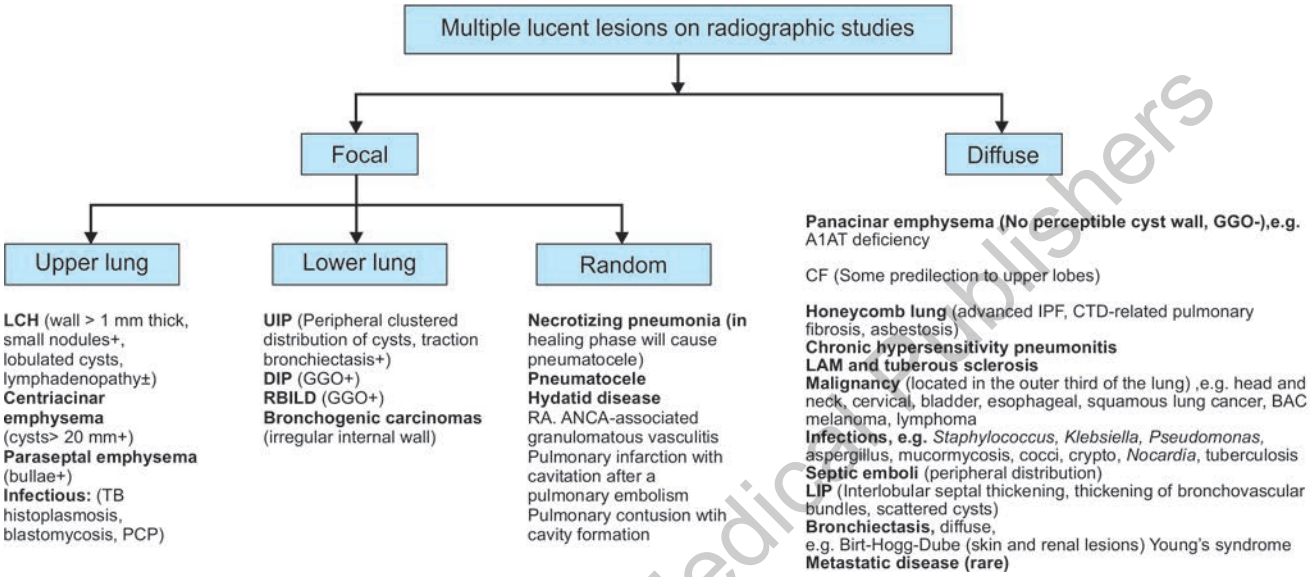

Abbreviations: LCH, Langerhans cell histiocytosis; TB, tuberculosis; PCP, *Pneumocystic jiroveci*; UIP, usual interstitial pneumonitis, DIP, desquamative interstitial pneumonitis; RBILD, respiratory bronchiolitis-interstitial lung disease; RA, rheumatoid arthritis; A1AT, alpha-1-antitrypsin; CF, cystic fibrosis; IFP, idiopathic pulmonary fibrosis; CTD, connective tissue disease; LAM, lymphangioleiomyomatosis; BAC, bronchoalveolar carcinoma; LIP, lymphocytic interstitial pneumonitis

the esophagus and lymph nodes. Abnormalities affecting the esophagus such as tumors, achalasia and Zenkers diverticulum are seen in this region. Vascular structures, such as an aberrant right subclavian, or thyroid masses, such as goiters, may also be seen in this area.[108]

Subcarinal Region

This region is situated below the carina and above the left atrium. Normal structures include fat, lymph nodes and the esophagus. The differential diagnosis of lesions in this location consists of lymphadenopathy, bronchogenic cysts, esophageal diverticulum or tumors **(Fig. 54)**.

Retrocardiac Clear Space

This retrocardiac space exists behind the heart and in front of the thoracic spine. Structures located in this space are the esophagus, aorta, azygous vein, fat, and lymph nodes. Esophageal lesions, such as duplication cyst, varices, hiatal hernia and tumor, aortic aneurysm and lymphadenopathy may arise in this location.

Fig. 54 CT chest (mediastinal window) demonstrating a large bronchogenic duplication cyst in the subcarinal region

Posterior Mediastinum

The posterior mediastinum covers the region posterior to the anterior border of vertebral bodies, where the vertebral

Fig. 55 CT chest showing insipation of bronchi in a patient with allergic bronchopulmonary aspergillosis

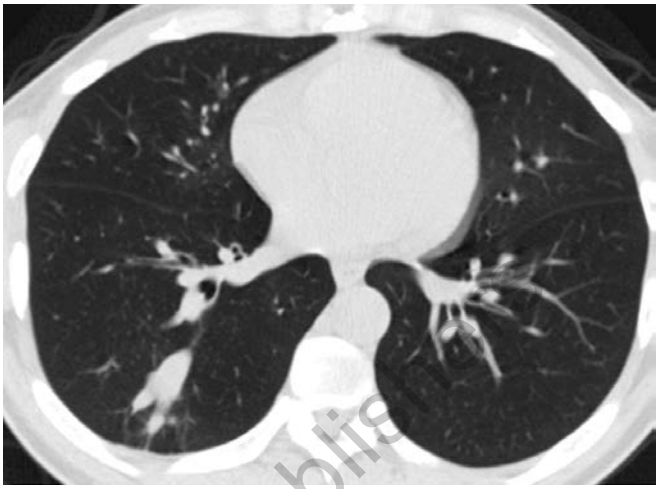

Fig. 56 CT chest in a patient with allergic bronchopulmonary aspergillosis showing insipation of the lower lobe bronchi

Fig. 57 CT chest with peripherally distributed opacities in a patient with chronic eosinophilic pneumonitis

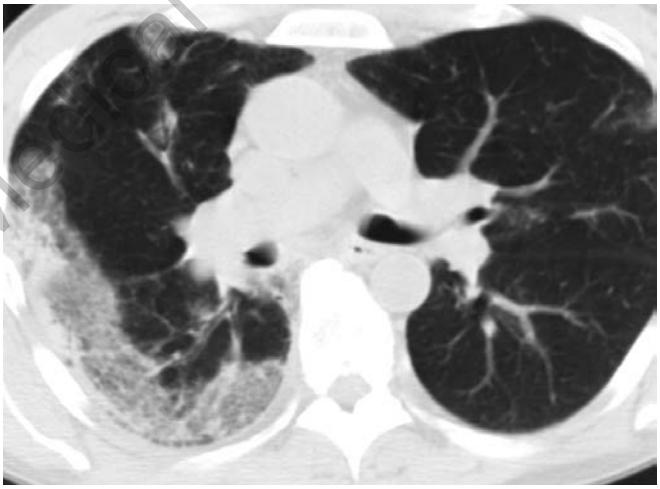

Fig. 58 CT chest in a patient with chronic eosinophillic pneumonitis with peripherally distributed opacities

column, fat and nerves are situated. The most common lesions in the posterior column are neurogenic and best imaged with MRI.

MISCELLANEOUS

Allergic Bronchopulmonary Mycosis

CT findings of ABPM include central airway abnormalities where there is bronchial dilatation with mucus-filled centrilobular bronchioles resulting in a tree-in-bud pattern **(Fig. 55)**.[109] Parenchymal abnormalities, such as consolidation, cavitation, bullae or scarring, and pleural abnormalities including focal pleural thickening may also be evident.[110] Central bronchiectasis and mucoid impaction are specific findings in ABPM **(Fig. 56)**.

Chronic Eosinophilic Pneumonia

The classic HRCT picture of chronic eosinophilic pneumonia is consolidation in a peripheral distribution confined primarily to the outer third of lung, and with an upper lobe distribution **(Figs 57 and 58)**.

Lipoid Pneumonia

CT findings of lipoid pneumonia have been studied in a small number of cases. In the appropriate clinical context, CT may demonstrate a solitary nodule resembling carcinoma, localized area of consolidation or extensive bilateral opacities.[111] HRCT findings of lipoid pneumonia show parenchymal nodules or opacities containing fat **(Fig. 59)**.

Fig. 59 CT chest representation of lipoid pneumonia

Fig. 60 CT chest showing diffuse fibrosis with ground glass attenuation in a patient with drug-induced lung disease

Drug-induced Lung Disease

There are several manifestations of drug-induced lung disease. The most common include noncardiogenic pulmonary edema, hypersensitivity pneumonitis and chronic pneumonitis.[112] Noncardiogenic pulmonary edema had been described to occur after administration of cytosine arabinoside, methotrexate and cyclophosphamide, resulting in a widespread airspace consolidation with predominance in the dependent lung regions. Hypersensitivity pneumonitis has been seen after methotrexate, cyclophosphamide and bleomycin administration. The HRCT finding consists of bilateral ground-glass attenuation in either patchy or diffuse distribution. Chronic pneumonitis is the most common drug-induced lung disease reported with all cytotoxic drugs which cause reticular changes in the lower lungs as seen with IPF **(Figs 60 and 61)**.

Fig. 61 CT chest showing diffuse fibrosis, increased density in drug-induced lung disease

CONCLUSION

The indications and role of CT imaging in the diagnoses of various thoracic diseases has been influenced immensely by a variety of technologic advancements. CT has become a fundamental part of clinical decision making in a number of conditions involving the lung parenchyma, airways, vasculature and mediastinum. Several characteristic features, such as ground-glass opacification, honeycomb changes and nodular features help to narrow down the differential diagnosis in many situations. These features depict the extent of disease processes and guide the course of management, eliminating the need for invasive diagnostic testing. It is, therefore, of paramount importance to understand and recognize the different CT features in thoracic conditions.

REFERENCES

1. Flohr TG, Schaller S, Stierstorfer K, Bruder H, Ohnesorge BM, Schoepf UJ. Multi-detector row CT systems and image-reconstruction techniques. Radiology. 2005;235(3):756-73.
2. Webb WR. Thin-section CT of the secondary pulmonary lobule: anatomy and the image—the 2004 Fleischner lecture. Radiology. 2006;239:322-38.
3. Müller NL. Clinical value of high-resolution CT in chronic diffuse lung disease. Am J Roentgenol. 1991;157:1163-70.
4. Heiken JP, Brink JA, Vannier MW. Spiral (helical) CT. Radiology. 1993;189(3):647-56.
5. Detterbeck FC, Mazzone PJ, Naidich DP, Bach PB. Screening for lung cancer: Diagnosis and management of lung cancer, 3rd edition. American College of Chest Physicians evidence-based clinical practice guidelines. Chest. 2013;143:e78S-92S.

6. Zerhouni EA, Naidich DP, Stitik FP, Khouri NF, Siegelman SS. Computed tomography of the pulmonary parenchyma: Part 2. Interstitial disease. J Thorac Imaging. 1985;1:54-64.
7. Weibel ER, Gill J. Structure–function relationships at the alveolar level. In: West JB (Ed). Bioengineering aspect of the lung. New York: Marcel Becker, Inc.; 1977. pp. 1-81.
8. Naidich DP, Zerhouni EA, Hutchins GM, Genieser NB, McCauley DI, Siegelman SS. Computed tomography of the pulmonary parenchyma: Part I: Distal air-space disease. J Thorac Imaging. 1985;1:39-53.
9. Miller WS. The Lung. Springfield: Charles C. Thomas; 1947.
10. Heitzman ER, Markarian B, Berger I, Dailey E. The secondary pulmonary lobule: a practical concept to an understanding of roentgen pattern in disease states. Radiology. 1969;93:514-20.
11. Raoof S, Amchentsev A, Vlahos I, Goud A, Naidich DP. Pictorial essay: mulitinodular disease; a high-resolution CT scan diagnostic algorithm. Chest. 2006;129:805-15.
12. Murata K, Itoh H, Todo G, Kanaoka M, Noma S, Itoh T, et al. Centrilobular lesions of the lung: demonstration by high-resolution CT and pathologic correlation. Radiology. 1986;161:641-5.
13. Austin JHM, Müller NL, Friedman PJ, Hansell DM, Naidich DP, Remy-Jardin M, et al. Glossary of terms for CT of the lungs: recommendations of the Nomenclature Committee of the Fleischner Society. Radiology. 1996;200:327-31.
14. Miller WT, Shah RM. Isolated diffuse ground-glass opacity in thoracic CT: causes and clinical presentations. Am J Roentgenol. 2005;184:613-22.
15. Leung AN, Miller RR, Müller NL. Parenchymal opacification in chronic infiltrative lung disease: CT-pathologic correlation. Radiology. 1993;188:209-14.
16. Foster WL, Pratt PC, Roggli VL, Godwin JD, Halvorsen RA, Putman CE. Centrilobular emphysema: CT-pathologic correlation. Radiology. 1986;159:27-32.
17. Stern EJ, Swensen SJ, Hartman TE, Frank MS. Pictorial assay. CT mosaic pattern of lung attenuation: Distinguishing different causes. Am J Roentgenol. 1995;165:813-6.
18. Naidich DP, Harkin TJ. Airways and lung: correlation of CT with fiberoptic bronchoscopy. Radiology. 1995;197:1-12.
19. Gamsu G, Webb WR. Computed Tomography of the trachea: normal and abnormal. Am J Roentgenol. 1983;18:51-60.
20. Breatnach E, Abbott GC, Fraser RC. Dimensions of the normal human trachea. Am J Roentgenol. 1984;141:903-6.
21. Stern EJ, Graham CM, Webb WR, Gamsu G. Normal trachea during forced expiration: dynamic CT measurements. Radiology. 1993;187:27-31.
22. Jackson CL, Huber JF. Correlated applied anatomy of the bronchial tree and lungs with a system of nomenclature. Chest. 1943;9:319-26.
23. Greene R. "Saber sheath" trachea: relation to chronic obstructive pulmonary disease. Am J Roentgenol. 1978;130:441-5.
24. Shin MS, Jackson RM, Ho KJ. Tracheobronchomegaly (Mounier-Kuhn syndrome): CT diagnosis. Am J Roentgenol. 1988;150:777-9.
25. Surprenant EL, O'Loughlin BJ. Tracheal diverticula and tracheobronchomegaly. Dis Chest. 1966;49:345-51.
26. Hartman T. Pearls and Pitfalls in Thoracic Imaging. New York, NY: Cambridge University Press; 2012. p. 234.
27. Restrepo S, Pandit M, Villamil MA, Rojas IC, Perez JM, Gascue A. Tracheobronchopathia osteochondroplastica: helical CT findings in 4 cases. J Thorac Imaging. 2004;19(2):112-6.
28. Baroni RH, Feller-Kopman D, Nishino M, Hatabu H, Loring SH, Ernst A, et al. Tracheobronchomalacia: comparison between end-expiratory and dynamic expiratory CT for evaluation of central airway collapse. Radiology. 2005; 235(2):635-41.
29. Kuriyama K, Gamsu G, Stern RG, Cann CE, Herfkens RJ, Brundage BH. CT-determined pulmonary artery diameters in predicting pulmonary hypertension. Invest Radiol. 1984;19: 16-22.
30. Elliot FM, Reid L. Some new facts about the pulmonary artery and its branching pattern. Clin Radiol. 1965;16:193-8.
31. Webb WR. Radiologic imaging of the pulmonary hila. Postgrad Radiol. 1986;6:145-68.
32. Sondheimer HM, Oliphant M, Schneider B, Kavey RE, Blackman MS, Parker FB Jr. Computerized axial tomography of the chest for visualization of "absent" pulmonary arteries. Circulation. 1982;65:1020-5.
33. Berden WE, baker DH, wung JT. Complete cartilage-ring tracheal stenosis associated with anomalous left pulmonary artery: the ring-sling complex. Radiology. 1984;152:57-64.
34. Dillon EH, Camputaro C. Partial anomalous pulmonary venous drainage of the left upper lobe vs duplication of the superior vena cava: distinction based on CT findings. AJR Am J Roentgenol. 1993;160:375-9.
35. Kuzo RS, Goodman LR. CT evaluation of pulmonary embolism: technique and interpretation. Am J Roentgenol. 1997;169: 959-65.
36. Tiegen CL, Maus TP, Sheedy PF, Johnson CM, Stanson AW, Welch TJ. Pulmonary embolism: diagnosis with electron-beam CT. Radiology. 1993;188:839-45.
37. Bartter T, Irwin RS, Nash G. Review: aneurysms of the pulmonary arteries. Chest. 1988;94:1065-79.
38. Borolowski GP, O'Donovan PB, Troup BR. Pulmonary varix: CT findings. J Comput Assist Tomogr. 1981;5:827-9.
39. Gudjberg CE. Roentgenologic diagnosis of bronchiectasis: an analysis of 112 cases. Acta Radiol. 1955;43:209-26.
40. Rosen M. Chronic Cough Due to Bronchiectasis ACCP Evidence-Based Clinical Practice Guidelines. Chest. 2006;129: 122S-31S.
41. Naidich DP. High resolution computed tomography of cystic lung disease. Semin Roentgenol. 1991;26:151-74.
42. Teel GS, Engeler CE, Tshijian JH, duCret RP. Imaging of small airways disease. Radiographics. 1996;16:27-41.
43. Devakonda A, Raoof S, Sung A, Travis WD, Naidich D. Bronchiolar disorders. A clinical-radiological diagnostic algorithm. Chest. 2010;137:938-51.
44. Hartman TE, Primack SL, Lee KS, Swensen SJ, Mueller NL. CT of bronchial and bronchiolar diseases. Radiographics. 1994;14:991-1003.
45. Im JG, Itoh H, Shim YS, Lee JH, Ahn J, Han MC, et al. Pulmonary tuberculosis: CT findings—early active disease and sequential change with antituberculous therapy. Radiology. 1993;186: 653-60.
46. Akira M, Kitatani F, Lee YS, Kita N, Yamamoto S, Higashihara T, et al. Diffuse panbronchiolitis: evaluation with high-resolution CT. Radiology. 1988;168:433-8.
47. Aquino SL, Gamsu G, Webb WR, Kee ST. Tree-in-bud pattern: frequency and significance on thin section CT. J Comput Assist Tomogr. 1996;20:594-9.
48. Bartter T, Irwin RS, Nash G, Balikian JP, Hollingsworth HH. Idiopathic Bronchiolitis obliterans organizing pneumonia

with peripheral infiltrates on chest roentgenogram. Arch Intern Med. 1989;149:273-9.
49. Epler GR, Colby TV, McLoud TC, Carrington CG, Gaensler EA. Idiopathic Bronchiolitis obliterans with organizing pneumonia. N Engl J Med. 1985;312:152-9.
50. Katzenstein ALA. Major problems in pathology. In: Katzenstein and Askin's surgical pathology of non-neoplastic lung disease, 3rd edition. Philadelphia: WB Saunders; 1997. p. 477.
51. Worthy SA, Flower CDR. Computed tomography of the airways. Eur Radiol. 1996;6:717-29.
52. Patel VK, Naik SK, Naidich DP, Travis WD, Weingarten JA, Lazzaro R, et al. A practical algorithm approach to the diagnosis and management of solitary pulmonary nodules: part 1: radiologic characteristics and imaging modalities. Chest. 2013;143(3):825-39.
53. MacMahon H, Austin JH, Gamsu G, Herold CJ, Jett JR, Naidich DP, et al. Guidelines for management of small pulmonary nodules detected on CT scans: a statement from the Fleischner Society. Radiology. 2005;237(2):395-400.
54. Munden RF, Pugatch RD, Liptay MJ, Sugarbaker DJ, Le LU. Small pulmonary lesions detected at CT: clinical importance. Radiology. 1997;202:105-10.
55. Libby DM, Henschke CI, Yankelevitz DF. The solitary pulmonary nodule: update 1995. Am J Med. 1995;99:491-6.
56. Swensen SJ, Silverstein MD, Ilstrup DM, Schleck CD, Edell ES. The probability of malignancy in solitary pulmonary nodules. Application to small radiologically indeterminate nodules. Arch Intern Med. 1997;157(8):849-55.
57. Bankoff MS, McEniff NJ, Bhadelia RA, Garacia-Moliner M, Daly BDT. Prevelance of pathologically proven intrapulmonary lymph nodes and their appearance on CT. Am J Roentgenol. 1996;167:629-30.
58. Furuya K, Murayama S, Soeda H, Murakami J, Ichinose Y, Yabuuchi H, et al. New classification of small pulmonary nodules by margin characteristics on high-resolution CT. Acta Radiol. 1999;40(5):496-504.
59. Zwirewich CV, Vedal S, Miller RR, Mueller NL. Solitary pulmonary nodule: hight-resoluation CT and radiologic-pathologic correlation. Radiology. 1991;179:469-76.
60. Primack SL, Hartman TE, Lee KS, Mueller NL. Pulmonary nodules and the CT halo sign. Radiology. 1994;190:513-5.
61. Gaeta M, Barone M, Russi EG, Volta S, Casablanca G, Romeo P, et al. Carcinomatous solitary pulmonary nodules: evaluation of the tumor-bronchi relationship with thin-section CT. Radiology. 1993;187:535-9.
62. Woodring JH, Fried AM. Significance of wall thickness in solitary cavities of the lung: a follow up study. Am J Roentgenol. 1983;140:473-4.
63. Mezaine MA, Hruban RH, Zerhouni EA, Wheeler PS, Khouri NF, Fishman EK, et al. High resolution CT of the lung parenchyma with pathologic correlation. Radiographics. 1988;8:27-54.
64. Nathan MH, Collins VP, Adama RA. Differentiation of benign and malignant pulmonary nodules by growth rate. Radiology. 1962;79:221-31.
65. O'Keefe Jr ME, Good CA, Mcdonald JE. Calcification in solitary nodules in the lung. Am J Roentgenol. 1957;77:1023-33.
66. Mahoney MC Sr, Shipley RT, Corcoran HL, Dickson BA. CT demonstration of calcification in carcinoma of the lung. Am J Roentgenol. 1990;154(2):255-8.
67. Siegelman SS, Khouri NF, Scott WW Jr, Leo FP, Hamper UM, Fishman EK, et al. Pulmonary hamartoma: CT findings. Radiology. 1986;160(2):313-7.
68. Littleton JT, Durizch ML, Moeller G, Herbert DE. Pulmonary masses: contrast enhancement. Radiology. 1990;177:861-71.
69. Swensen SJ, Brown LR, Colby TV, Weaver AL, Midthun DE. Lung nodule enhancement at CT: prospective findings. Radiology. 1996;201:447-55.
70. Ryu JH, Olson EJ, Midthun DE, Swensen SJ. Diagnostic approach to the patient with diffuse lung disease. Mayo Clin Proc. 2002;77:1221-7.
71. Katzenstein AL, Myers J. Idiopathic pulmonary fibrosis. Clinical relevance of pathologic classification. Am J Resp Crit Care Med. 1998;157:1301-15.
72. Thomeer M, Demedts M, Behr J, Buhl R, Costabel U, Flower CD, et al. Multidisciplinary interobserver agreement in the diagnosis of idiopathic pulmonary fibrosis. Eur Respir J. 2008;31(3):585-91.
73. Raghu G, Collard HR, Egan JJ, Martinez FJ, Behr J, Brown KK, et al. An official ATS/ERS/JRS/ALAT statement: idiopathic pulmonary fibrosis: evidence-based guidelines for diagnosis and management. Am J Respir Crit Care Med. 2011;183(6):788-824.
74. Müller NL, Miller RR, Webb WR, Evans KG, Ostrow DN. Fibrosing alveolitis: CT-pathologic correlation. Radiology. 1992;185:91-5.
75. Park JS, Lee KS, Kim JS, Park CS, Suh YL, Choi DL, et al. Nonspecific interstitial pneumonia with fibrosis: radiographic and CT findings in seven patients. Radiology. 1995;195:645-8.
76. Staples CA, Müller NL, Vedal S, Abboud R, Ostrow D, Miller RR. Usual interstitial pneumonias: correlation of CT with clinical, functional, and radiologic findings. Radiology. 1987;162:377-81.
77. Remy-Jardin M, Remy J, Cortet B, Mauri F, Delcambre B. Lung changes in rheumatoid arthritis: CT findings. Radiology. 1994;193:375-82.
78. Schurawitzki H, Stiglbauer R, Graninger W, Herold C, Pölzleitner D, Burghuber OC, et al. Interstitial lung disease in progressive systemic sclerosis: high-resolution CT versus radiography. Radiology. 1990;176:755-9.
79. Akira M, Yokoyama K, Yamamoto S, Higashihara T, Morinaga K, Kita N, et al. Early asbestosis: evaluation with high-resolution CT. Radiology. 1991;178:409-16.
80. Akira M, Yamatomo S, Yokoyama K, Kita N, Morinaga K, Higashihara T, et al. Asbestosis: high-resolution CT-pathologic correlation. Radiology. 1990;176:389-94.
81. Brauner MW, Grenier P, Mompoint D, Lenoir S, de Cremoux H. Pulmonary sarcoidosis: evaluation with high-resolution CT. Radiology. 1989;172:467-71.
82. Aikins A, Kanne JP, Chung JH. Galaxy sign. J Thorac Imaging. 2012;27:W164.
83. Müller NL, Kullnig P, Miller RR. The CT findings of pulmonary sarcoidosis: analysis of 25 patients. Am J Roentgenol. 1989;152:1179-82.
84. Lynch DA, Webb WR, Gamsu G, Stulbarg M, Golden J. Computed tomography in pulmonary sarcoidosis. J Comput Assist Tomogr. 1989;13:405-10.
85. Sider L, Horton ES. Hilar and mediastinal adenopathy in sarcoidosis as detected by computed tomography. J Thorac Imaging. 1990;5:77-80.
86. Remy-Jardin M, Degreef JM, Beuscart R, Voisin C, Remy J. Coal worker's pneumoconiosis: CT assessment in exposed workers and correlation with radiographic findings. Radiology. 1990;177:363-71.

87. Munk PL, Mueller NL, Miller RR, Ostrow DN. Pulmonary lymphangitic carcinomatosis: CT and pathologic findings. Radiology. 1988;166:705-9.
88. Silver SF, Mueller NL, Miller RR, Lefcoe MS. Hypersensitivity pneumonitis: evaluation with CT. Radiology. 1989;173:441-5.
89. Adler BD, Padley SP, Mueller NL, Remy-Jardin M, Remy J. Chronic hypersensitivity pneumonitis: high-resolution CT and radiographic features in 16 patients. Radiology. 1992;185:91-5.
90. Johkoh T, Muller NL, Pickford HA, Hartman TE, Ichikado K, Akira M, et al. Lymphocytic interstitial pneumonia: thin-section CT findings in 22 patients. Radiology. 1999;212(2):567-72.
91. Sugiyama Y. Diffuse panbronchiolitis. Clin Chest Med. 1993; 14(4):765-72.
92. Akira M, Kitatani F, Lee YS, Kita N, Yamamoto S, Higashihara T, et al. Diffuse panbronchiolitis: evaluation with high-resolution CT. Radiology. 1988;168(2):433-8.
93. Murata K, Takahashi M, Mori M, Kawaguchi N, Furukawa A, Ohnaka Y, et al. Pulmonary metastatic nodules: CT-pathologic correlation. Radiology. 1992;182:331-5.
94. Hartman TE, Primack SL, Swensen SJ, Hansell D, McGuinness G, Müller NL. Desquamative interstitial pneumonia: thin-section CT findings in 22 patients. Radiology. 1993;187:787-90.
95. Primack SL, Hartman TE, Ikezoe J, Akira M, Sakatani M, Müller NL. Acute Interstitial pneumonia: radiographic and CT findings in nine patients. Radiology. 1993;188:817-20.
96. Murch CR, Carr DH. Computed tomography appearance of pulmonary alveolar proteinosis. Clin Radiol. 1989;40:240-3.
97. Godwin JD, Müller NL. Pulmonary alveolar proteinosis: CT findings. Radiology. 1988;169:609-13.
98. Lee CH. The crazy-paving sign. Radiology. 2007;243:905-6.
99. Ujita M, Renzoni EA, Veeraraghavan S, Wells AU, Hansell DM. Organizing pneumonia: perilobular pattern at thin-section CT. Radiology. 2004;232(3):757-61.
100. Kim SJ, Lee KS, Ryu YH, Yoon YC, Choe KO, Kim TS, et al. Reversed halo sign on high-resolution CT of cryptogenic organizing pneumonia: diagnostic implications. Am J Roentgenol. 2003;180(5):1251-4.
101. Trigaux JP. Gevenois PA, Goncette L, Gouat F, Schumaker A, Weynants P. Bronchioloalveolar carcinoma: computed tomography findings. Eur Respir J. 1996;9(1):11-6.
102. Seaman D, Meyer C. Diffuse cystic lung disease at high-resolution CT. Am J Roentgenol. 2011;196:1305-11.
103. Müller NL, Chiles C, Kullnig P. Pulmonary lymphangiomyomatosis: correlation of CT with radiographic and functional findings. Radiology. 1990;175:335-9.
104. Brauner MW, Grenier P, Mouelhi MM, Mompoint D, Lenoir S. Pulmonary histiocytosis X: evaluation with high resolution CT. Radiology. 1989;172:255-8.
105. Bergin CJ, Wirth RL, Berry GJ, Castellino RA. *Pneumocystis carinii* pneumonia: CT and HRCT observations. J Comput Assist Tomogr. 1990;14:756-9.
106. Morgenthaler TI, Brown LR, Colby TV, Harper CM, Coles DT. Thymoma. Mayo Clinic Proc. 1993;68:1110-23.
107. Hoffman OA, Gillespie DJ, Aughenbaugh GL, Brown LR. Primary mediastinal neoplasms (other than thymomas). Mayo Clin Proc. 1993;68:880-91.
108. Franquet T, Erasmus JJ, Giménez A, Rossi S, Prats R. The retrotracheal space: normal anatomic and pathologic appearances. Radiographics. 2002;22:S231-46.
109. Neeld DA, Goodman LR, Gurney JW, Greenberger PA, Fink JN. Computerized tomography in the evaluation of allergic bronchopulmonary aspergillosis. Am Rev Respir Dis. 1990;142: 1200-6.
110. Panchal N, Bhagat R, Pant C, Shah A. Allergic bronchopulmonary aspergillosis: the spectrum of computed tomography appearances. Respir Med. 1997;91:213-9.
111. Wheeler PS, Stitik FP, Hutchins GM, Klinefelter HF, Siegelman SS. Diagnosis of lipoid pneumonia by computed tomography. JAMA. 1981;235:65-6.
112. Padley SPG, Adler B, Hansell DM, Müller NL. High resolution computed tomography of drug induced lung disease. Clin Radiol. 1992;46:232-6.